Acta Biomaterialia 208 (2025) 428–441

Contents lists available at ScienceDirect

Acta Biomaterialia

journal homepage: www.elsevier.com/locate/actbio

Full length article

Comparison of biofilm-degrading activities of two glycoside hydrolase family 20 enzymes against clinical and veterinary β-1,6-poly-N-acetyl-D-glucosamine-dependent *Staphylococcus aureus* isolates

Andrei Nicoli Gebieluca Dabul [a,†], Lorgio Victor Bautista Samaniego [b,†], Anelyse Abreu Cortez [b], Samuel Luis Scandelau [b], Marcelo Vizoná Liberato [b], Agatha MS Kubo [c], Ana Beatriz Rodrigues [d], Rejane MT Grotto [c], Guilherme Valente [d], Vera Lúcia Mores Rall [e], Sebastião Pratavieira [b], Mario de Oliveira Neto [e], Carla Raquel Fontana [a], Igor Polikarpov [b,*]

[a] School of Pharmaceutical Sciences, São Paulo State University, Rodovia Araraquara-Jáu, km 1, 14800-903, Araraquara, SP, Brazil
[b] São Carlos Institute of Physics, University of São Paulo, poloTErRA, Avenida João Dagnone, 1100, 13563-120, São Carlos, SP, Brazil
[c] School of Agriculture Sciences, Sao Paulo State University, Experimental Lageado Farm, 18610-034, Botucatu, SP, Brazil
[d] Clinical Hospital of Medicine School of Sao Paulo State University, District of Rubiao Jr., 18618-687, Botucatu, SP, Brazil
[e] Institute of Biosciences, Sao Paulo State University, District of Rubiao Jr., 18618-970, Botucatu, SP, Brazil

ARTICLE INFO

Keywords:
Biofilms
Staphylococcus aureus
Glycoside Hydrolases
Antimicrobial resistance

ABSTRACT

Biofilms shield microbial communities from various environmental threats, including antimicrobial agents. Such protection renders bacterial cells within biofilms more resistant to antimicrobial agents than their planktonic counterparts. Degradation of the exopolysaccharides of the biofilm matrix using glycoside hydrolases (GH) strongly increases the efficacy of antimicrobials against biofilms. *Staphylococcus aureus* is a leading cause of infections in both humans and animals, with many of its strains producing biofilms rich in β-1,6-N-acetyl-D-glucosamine (PNAG), the primary component of the extracellular matrix of their biofilms. In this study, we recombinantly produced and biochemically characterized two glycoside hydrolases from GH20 family, *Ap*GH20 and *Ch*GH20, both of which specifically target PNAG. These enzymes effectively degraded and inhibited biofilm formation of *S. aureus* human clinical strain which produces a robust PNAG-based biofilm. Both enzymes also demonstrated high activity against several veterinary *S. aureus* isolates. All of these isolates have been sequenced and analyzed. Notably, *Ap*GH20 exhibited nearly three orders of magnitude higher activity than *Ch*GH20 in degrading *S. aureus* biofilm, yet both enzymes similarly enhanced the ability of gentamicin to kill human isolate of *S. aureus*, albeit at different dosages. These findings further demonstrate that application of glycoside hydrolases, when combined with antimicrobial agents, is a promising strategy for treating infections caused by pathogenic *S. aureus* strains.

Statement of Significance: Antimicrobial resistance is a very significant health problem, resulting in millions of deaths worldwide. Pathogenic bacteria become resistant to antibiotics using various mechanists, one of which is to protect themselves by biofilms. *Staphylococcus aureus* is a leading cause of infections in both humans and animals, with many of its strains relying on β-1,6-N-acetyl-D-glucosamine (PNAG) polysaccharide as an important part of their biofilms. Here we produced two glycoside hydrolase enzymes which specifically target PNAG. We showed that the enzymes effectively degraded and also prevented biofilm formation of *S. aureus* human clinical and several veterinary isolates. Both enzymes similarly enhanced efficiency of gentamicin against

* Corresponding author.
E-mail address: ipolikarpov@ifsc.usp.br (I. Polikarpov).
† The first two authors contributed equally to this work.

https://doi.org/10.1016/j.actbio.2025.10.032
Received 26 May 2025; Received in revised form 5 October 2025; Accepted 16 October 2025
Available online 17 October 2025

S. aureus, albeit at different dosages, which might hold promise to treat infections caused by these pathogenic bacteria.

1. Introduction

Staphylococcus aureus is one of the most prevalent human pathogens leading to severe infections worldwide. It is associated with a very high mortality rate, accounting for over 1 million of the 13.7 million infection-related deaths in 2019 [1]. Infections caused by *S. aureus* include pneumonia and other respiratory tract infections, cardiovascular infections, infections of prosthetic joints, and nosocomial bacteremia, to name a few [2].

The pathogenicity of this bacterium can be attributed to its wide array of virulence factors, which allow it to evade phagocytosis, invade tissues, and persist at infection sites [2]. Among these mechanisms, biofilm formation plays a crucial role, providing protection of microbial cells from hostile environments, including the human immune system [3].

Biofilms are defined as communities of microorganisms embedded in a self-produced extracellular matrix composed of proteins, extracellular DNA, polysaccharides, and other biomolecules [3]. Several genes are associated with biofilm production across different microorganisms. In *Staphylococcus* species, the *ica* operon, which consists of four genes, is responsible for the synthesis of the polysaccharide intercellular adhesin (PIA), a polymer of partially deacetylated β-(1,6)-poly--N-acetyl-D-glucosamine (PNAG) [3]. In other genera, a similar polymer is produced by a different operon, such as *pgaABCD*, in *E. coli* [4].

Currently, various strategies are being developed aiming to degrade bacterial biofilms, including the use of glycoside hydrolases [5–7]. This strategy is particularly effective due to the high specificity of glycoside hydrolases for the polymers they hydrolyze. As long as the main component of the biofilm is a polysaccharide, an appropriate glycoside hydrolase can be selected to degrade the polysaccharide. This concept was first demonstrated by Kaplan et al. (2003) using Dispersin B, a GH20 glycoside hydrolase from *Aggregatibacter actinomycetemcomitans*. In their study, the authors analyzed transposon insertion mutants of this bacterium, known for its robust biofilms, and found that one mutant was unable to detach from the biofilm and form new colonies. The transposon was found to be inserted into a novel gene, named *dspB*, encoding an N-acetylglucosaminidase [8]. At least 32 orthologs of the *dspB* gene have been identified in bacteria, primarily among the families *Pasteurellaceae* and *Neisseriaceae* [9].

Dispersin B from both *A. actinomycetemcomitans* and *Actinobacillus pleuropneumoniae* has been reported to detach preformed biofilms of *A. actinomycetemcomitans, A. pleuropneumoniae*, and *Staphylococcus epidermidis*, as these organisms share the same primary extracellular matrix component, PNAG, which Dispersin B specifically hydrolyses [4,8,10].

There is a growing interest in enzymatic strategies for disrupting pathogenic bacterial biofilms, including those of *S. aureus*. Establishing of such technologies in applied settings requires extensive studies of new and novel enzyme capable of *S. aureus* biofilm exopolysaccharide degradation, notably GH20 glycoside hydrolases. Although discovery of Dispersin B has been a notable achievement in this area, a large amount of its orthologs discovered in recent genomics studies provide a fertile ground for further advances in this field. We feel that without further studies of PNAG-active enzymes, including the ones from GH20 family, it would be difficult, if not impossible to discover new enzymatic catalysts which can be used for enzymatic degradation of PNAG-rich *S. aureus* biofilms.

Thus, in the present study, we conducted structural and biochemical characterization of two Dispersin B orthologs, *Ap*GH20, from *A. pleuropneumoniae* and *Ch*GH20, from *Cardiobacterium hominis* and investigated their ability, to degrade and also to inhibit biofilm formation of both veterinary and human *S. aureus* pathogenic isolates. We have also assessed their combined action with gentamicin in an effort to overcome antimicrobial resistance of *S. aureus* biofilms.

2. Materials and methods

2.1. Bacterial strains

S. aureus 03 is a human clinical isolate and *S. aureus* MSA22, MSA29, MSA36, MSA89 and MSA90 are veterinary isolates associated with bovine mastitis. All the isolates originate from the Sao Paulo state, Brazil.

The veterinary isolates of *S. aureus* were obtained from milk samples collected from mammary gland quarters of cows with mastitis (positive California Mastitis Test). The milk samples were plated onto sheep blood agar (5 %) and characteristics colonies were identified through traditional methodology according to Procop et al. (2020) [11]. The colonies were confirmed by the presence of the *nuc* gene (CRL-AR, 2009). (Ethics Committee on Animal Use in the School of Veterinary Medicine and Animal Science, São Paulo State University, Botucatu, N° 2015/19688-8)

2.2. Genome sequencing

S. aureus strains 03, MSA22, MSA29, and MSA90 were cultured overnight on Mannitol Salt Agar (BD Difco™, USA). The colonies were then isolated and transferred to Brain Heart Infusion (BHI) broth (BD Difco™, USA) for a second overnight incubation. One milliliter of the culture was centrifuged, and 850 μL of the supernatant was discarded. The remaining pellet was incubated with 50 μL of lysozyme (25 mg/mL) for 15 min under agitation. Bacterial DNA was extracted using the Stool DNA Isolation Kit (Norgen Biotek, Canada) in spin column format and stored at -80°C according to the manufacturer's instructions. Genomic libraries were prepared using the Illumina DNA Prep (Illumina, USA) and sequenced with the MiSeq Reagent Micro Kit v2 flow cell (Illumina, USA) for 300 cycles, following the manufacturer's guidelines.

The sequencing reads were initially evaluated for quality using FASTQC software (Babraham Institute, 2024). Adapter removal and trimming of low-quality regions were carried out using Trimmomatic [12]. After processing, the reads were reassessed with FASTQC, and the unpaired reads were combined into a single file for assembly.

The initial genome assembly was performed using Unicycler [13] with default settings. The assembly was further refined using RagTag [14], which scaffolded the assemblies with a reference genome from RefSeq: *Staphylococcus aureus* (ASM1672758v1).

S. aureus genomes assembled have ~2,6 Mb of total length, which were assembled onto up to 5 contigs, with a N50/90 ~2.6 Mb, L50/90 of 1, GC content ~32 %, and coverage >99 % (Supplementary Table 1). These metrics indicate that we obtained desirable sequences and assemblies.

The human isolate *S. aureus* 03 underwent genotypic characterization following the acquisition of its draft genome sequence using Illumina sequencing. The genome was annotated using Rapid Annotation using Subsystem Technology (RAST) [15] and was typed with MLST 2.0, SCC*mec*Finder 1.2, *spa*Typer 1.0 and PlasmidFinder 2.1, all available through the Center for Genomic Epidemiology (CGE) website (https://www.genomicepidemiology.org/). Additionally, it was phenotyped with ResFinder 4.6.0 and VirulenceFinder 2.0, also available through CGE website, along with CARD [16]. The potential resistance profile was confirmed phenotypically with Etest® (Biomérieux, Marcy-l'Étoile, France) for vancomycin, broth microdilution for gentamicin, and disk diffusion for chloramphenicol, cefoxitin, rifampin, trimethoprim,

erythromycin, norfloxacin, tetracycline, and penicillin G, adhering to the criteria established by the Clinical and Laboratory Standards Institute [17]. *S. aureus* ATCC 25923 and *Escherichia coli* ATCC 25922 were used as quality control strains for antimicrobial susceptibility testing. A phylogenetic tree was constructed with REALPHY to verify the relationship of *S. aureus* 03 to the main *S. aureus* lineages [18].

The veterinary isolates were subjected to adjusted assembly annotation using Prokka [19] and assessed for quality and consistency with QUAST [20]. Comparative analyses were conducted using the BLAST tool against the reference genome *S. aureus* ASM1672758v1, and genome annotation was performed with Prokka. Both analyses were carried out directly within the Proksee platform, and the resulting annotations were incorporated into the circular genome visualizations.

2.3. Cloning and protein expression

The gene encoding *Ch*GH20 (WP_082159814) was cloned from the genomic DNA of *Cardiobacterium hominis* DSM 8339 into pETTRX1a/LIC using a Ligation Independent Cloning technique as previously described [21]. The protein of interest was expressed in *E. coli* BL21 Rosetta.

The gene encoding *Ap*GH20 was synthesized based on the genome of *A. pleuropneumoniae* following *in silico* optimization for expression in *E. coli*. The gene was subsequently cloned into pETTRX1a/LIC, as described above, and the protein of interest was expressed in *E. coli* BL21 Rosetta.

For protein expression, each transformant was cultivated in 5 mL of LB broth supplemented with 50 mg/L kanamycin and 34 mg/L chloramphenicol, under agitation at 37°C overnight. Subsequently, each preinoculum was transferred to 1 L of LB broth and cultured under agitation at 37°C until the optical density at 600 nm reached 0.5. The temperature was then reduced to 20°C, and the protein expression was induced with 1 mM IPTG overnight.

2.4. Purification of enzymes

The bacterial cultures were centrifuged at 13,000 g for 20 min at 4 °C. The resulting pellet was resuspended in 50 mL of lysis buffer (50 mM Tris-HCl, 300 mM NaCl, 250 μg/mL lysozyme, and 2 mM phenylmethylsulfonyl fluoride (PMSF)) and froze at -20°C. After thawing, the pellet was lysed by subjecting it to 10 cycles of sonication for 30 s followed by 30 s of rest, all performed on an ice bath. The solution was then centrifuged at 13,000 g for 20 min at 4 °C.

Protein purification was carried out using bench-top columns packed with 5 mL Ni Sepharose™ 6 Fast Flow resin (GE Healthcare®), which was equilibrated with 50 mM Tris-HCl, 100 mM NaCl, and 10 mM imidazole. All chemicals used were sourced from Sigma-Aldrich®. The column wash buffer was the same as the equilibration buffer. Proteins were eluted in 20 mL of buffer containing 300 mM imidazole, and the column was subsequently cleaned with 40 mL of buffer containing 500 mM imidazole to remove impurities.

The purified fractions were analyzed by SDS-PAGE. The buffer was then gradually exchanged for 20 mM Tris-HCl and 100 mM NaCl using a 10 kDa molecular weight Amicon® Pro Purification cellulose concentrator (Merck®). Following purification, the TRX+His6 tag of the enzymes was cleaved using Tobacco Etch Virus (TEV) protease. The cleavage was performed at 4°C for 46 h with constant homogenization, using a 1:10 ratio of TEV protease to enzyme. The mixture was then loaded onto the same nickel column setup to collect the flow-through containing the cleaved GH20s. Protein concentration was determined using NanoDrop™ 2000 Spectrophotometer (Thermo Scientific®) at 280 nm (*Ap*GH20, theoretical mass = 40.38 kDa, $\varepsilon = 57.3\ M^{-1}\ cm^{-1}$; *Ch*GH20, theoretical mass = 39.75 kDa, $\varepsilon = 49.85\ M^{-1}\ cm^{-1}$, as predicted by ProtParam). Finally, all enzymes were sterilized by syringe membrane filtration (0.22 μm).

2.5. Biochemical characterization and structural analysis of GH20 enzymes

The optimal pH and temperature of two GH20 enzymes were determined. For all assays, 4-nitrophenyl N-acetyl-β-D-glucosaminide (pNP-NAG) at a concentration of 4 mM was used as the substrate. 4-nitrophenyl-linked sugars are artificial substrates commonly used to study enzyme kinetics. This approach relies on the release of the chromogenic compound p-nitrophenol following hydrolytic cleavage. Such substrates have been widely applied to investigate glycoside hydrolases from various families, including GH20 [22–25]. The method is particularly useful when no natural or commercially available substrate exists for the enzyme of interest, as in the case of PNAG. Since Dispersin B, the most extensively studied GH20 member, has been reported to catalyze both endo- and exo-glycosidic cleavage depending on the nature of the substrate [9], we employed the pNP-NAG assay to determine the kinetic parameters of *Ap*GH20 and *Ch*GH20.

The reaction mixture had a total volume of 100 μL, containing the appropriate amounts of enzyme and substrate. All reactions, except for those testing temperature activity, were performed at 37°C for 30 min, with the reaction terminated by adding 100 μL of 1 M sodium carbonate solution. The release of p-nitrophenol was quantified by measuring absorbance at 410 nm, using a standard curve. Sodium citrate buffer at pH 5 and phosphate buffer at pH 7 were used for pNP-NAG-based assays.

To determine the optimal temperature, the enzymes were tested in the range of 30 to 55 °C using pNP-NAG as the substrate in a solution containing 50 mM sodium citrate buffer at pH 5. The optimal pH of the enzymes was evaluated by incubating the proteins for 30 min in a 20 mM acetate/borate/phosphate (ABF) buffer across a pH range of 2 to 10 at 37 °C.

The structures of *Ap*GH20 and *Ch*GH20 were predicted using the ColabFold online server [26]. All molecular representations, including surface and electrostatic potential maps, were generated with PyMOL software (The PyMOL Molecular Graphics System, Version 1.8, Schrödinger, LLC, New York, NY, USA). Structural alignments of the studied GH20 enzymes were performed in PyMOL using the crystal structure of Dispersin B (PDB: 1YHT) [27] as a reference. Primary sequence alignments were conducted in MEGA X [28] and visualized using ESPript3 [29].

2.6. Degradation of preformed S. aureus biofilms

To evaluate the ability of the enzymes to degrade preformed biofilms, *S. aureus* biofilms were cultivated as follows: A five milliliters preinoculum was cultivated at 37°C for 16 h, and then adjusted to OD_{600}=0.1, which corresponds to 1×10^8 CFU/mL, followed by a 1:10 dilution in TSB + 0.75 % glucose. This inoculum (1×10^7 CFU/mL) was distributed in the wells of a flat bottom tissue culture 96-well plate (Kasvi, São José dos Pinhais, Brazil), 200 μL per well. The wells on the borders were filled only with culture medium to avoid evaporation and to serve as sterility controls. The microplate was incubated at 37 °C for 24 h, the expended culture medium together with the planktonic cells were aspirated and discarded, and the remaining biofilm at the bottom was subjected to three washes with saline solution.

Two hundred microliters of the enzymes (*Ap*GH20 or *Ch*Gh20) diluted in 20 mM Tris-HCl, pH 8 and 100 mM NaCl buffer were then applied to the biofilms in the following concentrations: 5, 50, and 500 mg/L. Buffer-only wells served as treatment control. The microplates were maintained at 37°C for either 30 min, 1, 2 or 4 h. Each experimental condition was tested in six replicates and on three different occasions.

Following the treatment, the solutions were removed from the wells of the microplate, and the remaining biofilms were washed thrice with saline, and the biofilm biomass was stained with 200 μL of a 0.5 % Crystal Violet solution. After five minutes at room temperature, the dye solution was removed, the wells were washed thrice with saline and then

filled with 200 μL of 30 % acetic acid solution to destain the biofilm-bound dye. After five minutes at room temperature, 100 μL of the wells' content were transferred to a new 96-well flat bottom microplate and subjected to absorbance reading at 595 nm in a Synergy H1 Microplate Reader (Biotek, Winooski, USA).

2.7. Inhibition of production of S. aureus 03 biofilm

The capacity of the enzymes to inhibit the formation of *S. aureus* 03 biofilm was evaluated as follows. A five milliliters *S. aureus* 03 pre-inoculum was cultivated at 37 °C for 16 h, and then it was adjusted to OD_{600}=0.1, corresponding to 1×10^8 CFU/mL. The enzymes were prepared as 10x stocks (50, 500, and 5000 mg/L) in 20 mM Tris-HCl, pH 8 and 100 mM NaCl buffer. Then, the wells of a flat bottom tissue culture 96-well plate were filled with 160 μL of TSB + 0.75 % glucose, 20 μL inoculum, and 20 μL of each enzyme stock solution (*Ap*GH20 or *Ch*GH20) so that the inoculum reached 1×10^7 CFU/mL and the enzymes reached 5, 50 or 500 mg/L in the final volume of the well. A set of wells with only buffer instead of enzyme solution served as treatment control. The wells on the borders were filled only with culture medium to avoid evaporation and to serve as sterility controls. Each experimental condition was tested in six replicates on three different occasions.

The microplate was incubated at 37 °C for 24 h, the expended culture medium together with the planktonic cells were aspirated and discarded, and the remaining biofilm at the bottom was subjected to three washes with saline. After that, the biofilm biomass was measured using Crystal Violet staining as described above.

2.8. Combined antimicrobial treatment

In order to test if the action of the enzymes improves the efficiency of antimicrobials on *S. aureus* 03 biofilm, we used a combined treatment strategy applying either *Ap*GH20 or *Ch*GH20 together with gentamicin to the biofilms. For this, the biofilms were cultured as described for the Degradation of Preformed Biofilm experiment, then were subjected to three washes with saline. Based on previous dose-response assays, fixed concentrations of 20 mM Tris-HCl, pH 8 and 100 mM NaCl diluted *Ap*GH20 (50 mg/L) and *Ch*GH20 (500 mg/L) were selected for pre-treatment, being 200 μL per well. The microplate was maintained at 37 °C for 1 h and then the wells were washed thrice with saline. The same pretreatment was performed in parallel using only the buffer where the enzymes were diluted, to serve as a control.

After that, 200 μL of gentamicin diluted in Mueller-Hinton broth was applied in the following concentrations, in triplicate (for both biofilms – pretreated with enzyme and pretreated with buffer): 0, 0.03125, 0.0625, 0.125, 0.25, 0.5, 1, 2, 4, and 8 mg/L. The microplate was incubated at 37°C for 24 h. A hundred microliters of the content of each well were transferred to a 96-well black flat bottom microplate, and to each well was added 20 μL of a 0.15 mg/mL resazurin solution. The microplate was kept at 37°C for 2 h and the wells contents had their fluorescence measured in a Synergy H1 Microplate Reader with excitation at 550 nm and emission at 590 nm, to verify the viability of bacterial cells [30].

2.9. Confocal microscopy analyses

For confocal microscopy experiments, we followed the same biofilm formation workflow as described above, with the exception of the final volume per well. In this case, 1 mL was used to fill the wells of a 24-well plate (Kasvi, São José dos Pinhais, Brazil) which was incubated at 37°C for 24 h. After washing, 500 μL of a treatment solution containing 50 mg/L of *Ap*GH20 or *Ch*GH20 (diluted in 20 mM Tris-HCl, pH 8, and 100 mM NaCl buffer) was applied. For the control, only the dilution buffer was used.

After treatment, two independent fluorescent staining protocols were performed. To assess biofilm viability, the LIVE/DEAD™ BacLight™ Bacterial Viability Kit for microscopy (Invitrogen, Carlsbad, USA) was used according to the manufacturer's instructions. For carbohydrate and protein identification, a two-step staining procedure was employed. First, biofilms were stained with Calcofluor White Stain solution (10 μg/mL) (Sigma-Aldrich, St. Louis, USA), followed by FilmTracer™ SYPRO® Ruby Biofilm Matrix Stain (Invitrogen, Carlsbad, USA), as described in our previous studies [31].

These samples were analyzed using a fluorescence confocal microscope (Zeiss LSM 780, Oberkochen, Germany) equipped with an EC Plan-Neofluar 10×/0.30 M27 objective. Images were acquired at a resolution of 512 × 512 pixels, covering a scanning area of 850.2 μm × 850.2 μm. All control (untreated) and low-degradation samples were imaged using a Z-stack depth greater than 200 μm, enabling 3D reconstruction. In contrast, images from successful enzymatic treatments were acquired without Z-stacking due to low fluorescence intensity at the z-axis. Additionally, the arithmetic mean fluorescence intensity was calculated from the middle plane of the Z-stack (when applicable), based on the statistical values derived from the fluorescence histograms of all CLSM images.

2.10. Statistical methods

Statistical evaluations were carried out utilizing Prism 5. One-way analysis of variance with a Tukey post-test was conducted with the results of the experiments of Degradation of preformed *S. aureus* biofilms and Inhibition of production of *S. aureus* biofilms, which were plotted as mean ± standard deviation. Results were considered statistically significant when P-value < 0.01. For the Gentamicin effect after enzymatic pre-treatment of biofilms, Two-way analysis of variance with Bonferroni's post hoc was conducted, and the differences between groups were considered statistically significant when P-value < 0.001.

3. Results

3.1. Characterization of the human infection isolate S. aureus 03

The draft genome sequence of *S. aureus* 03 consists of one contig of 2,598,718 bp, corresponding to its chromosome, one contig of 20,731 bp, corresponding to a plasmid, and four additional contigs, each smaller than 3,500 bp. Annotation using RAST revealed 2,439 coding sequences and 59 RNAs (Fig. 1a). The strain was assigned to sequence type (ST) 8, although one of the seven alleles, *aroE*, exhibited a single nucleotide polymorphism. The genome does not contain an SCC*mec* element, as the strain is not methicillin-resistant, and therefore, no SCC*mec* type could be assigned. Additionally, the strain was identified as *spa* type t008.

Several virulence genes were identified in the *S. aureus* 03 genome, including those encoding γ-hemolysin (*hlgA, hlgB* and *hlgC*), leukocidins (*lukD* and *lukE*), aureolysin, and serine proteases (*splABCDEF*).

Plasmid replicons identified by PlasmidFinder 2.1 included *rep*5a and *rep*16, which were found in the 20,731 bp contig. This contig also harbored genes conferring resistance to cadmium, as well as the *blaZ* gene, which provides resistance to beta-lactams. This plasmid shares similarity with pSaa6159, a member of the Inc18 family [32]. One of the smaller contigs (<3.500 bp) contained the replication gene *rep*10b, although no other significant hits were detected. The contig corresponding to the chromosome (2,598,718 bp) contained the *rep*7c gene, which may have resulted from an early integration event.

The ResFinder 4.6.0 database search identified only the *blaZ* gene in the *S. aureus* 03 genome, which could confer resistance to beta-lactams. This was confirmed through a Penicillin G disk diffusion test. Furthermore, the CARD database detected perfect matches to several efflux pump-related genes, including *lmrS* (macrolides, aminoglycosides, oxazolidinones, diaminopyrimidines and phenicols), *alrR* and *alrS* (fluoroquinolones and antiseptics), *mgrA* (fluoroquinolones, cephalosporines, penams, tetracyclines, peptides and antiseptics), *mepA and mepR* (glycylcyclines and tetracyclines), *sdrM* (fluoroquinolones and

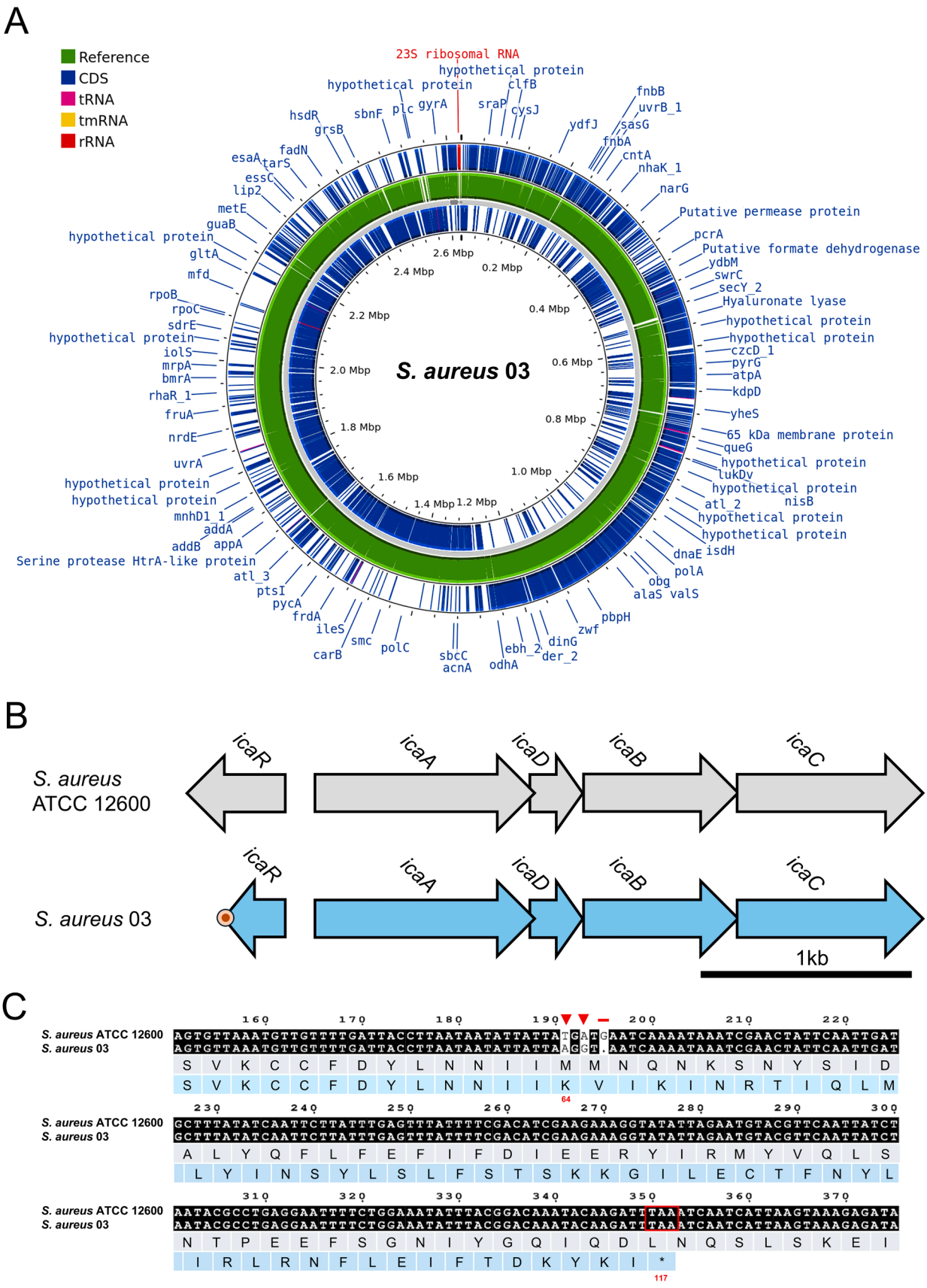

Fig. 1. Genome analysis of *S. aureus* 03 strain. A- Circular genome representation, including selected gene annotations and functions. B - Comparison of the *ica* operon between *S. aureus* ATCC 12600 (reference genome: ASM1672758v1) and *S. aureus* 03. C - Sequence alignment highlighting the mutation in the *ica*R gene of *S. aureus* 03.

antiseptics) and *sepA* (antiseptics). However, despite the presence of *lmrS*, the strain was susceptible to chloramphenicol, trimethoprim, and erythromycin, as indicated by disk diffusion, and to gentamicin (MIC = 0.25 mg/L), as determined by broth microdilution. Similarly, resistance to norfloxacin was not observed despite the presence of *mgrA* and *sdrM*, nor to tetracycline, despite the presence of *mepA* and *mepR*. According to Etest, the strain was also susceptible to vancomycin (MIC = 1.5 mg/L). In addition to beta-lactam resistance, the only resistance detected *in silico* that was confirmed *in vitro* was to rifampin, due to a mutation (H481N) in *rpoB* detected by CARD.

The complete *ica* operon (*icaADBC* genes) was identified in the strain's genome, confirming the biofilm produced by this strain contains PNAG and thus can be degraded by *Ap*GH20 and *Ch*GH20. Additionally, the strain exhibited a mutation in the *icaR* gene due to the deletion of a guanine at position 195, which caused a frameshift, resulting in a premature stop codon (Fig. 1b,c). This mutation truncated the expressed IcaR, a negative regulator protein, from 186 to 116 amino acid residues, leading to abundant expression of PNAG.

3.2. ApGH20 and ChGH20 production and characterization

Both GH20 enzymes were successfully cloned and expressed in their TRX-6His fused forms, with an approximate molecular weight of 54 kDa (Supplementary Figure S1). A single step of nickel affinity chromatography was sufficient to purify the enzymes. After treatment with TEV protease, the non-fused versions of GH20 had approximate molecular weights of 40.4 kDa for *Ap*GH20 and 39.8 kDa for *Ch*GH20.

Several biochemical characteristics of the enzymes were assessed using the pNP-NAG substrate. Both enzymes exhibited the highest activity within the temperature range of 35–40°C (Supplementary Figure S2). This optimal temperature is expected, as these enzymes originate from mesophilic pathogens. Additionally, the enzymes remained active at 45°C, retaining at least 50 % of their enzymatic activity. The optimal pH for *Ap*GH20 was 7, while for *Ch*GH20, it was 5 (Supplementary Figure S3). However, both enzymes retained more than 60 % of their activity at pH 6. Despite the optimal pH for *Ch*GH20 being 5, we observed that the enzyme was unstable at this pH, with a very short shelf life. In contrast, when the enzymes were maintained in their purification buffer (pH 8), both remained stable for several weeks, while still active (Supplementary Figure S3). Therefore, biofilm experiments were performed using a 20 mM Tris-HCl, pH 8, 100 mM NaCl buffer.

3.3. ApGH20 and ChGH20 enzymatic degradation of S. aureus biofilms

Remarkably, almost complete degradation of *S. aureus* 03 biofilm was achieved with any of the tested concentrations of *Ap*GH20, even with the shortest time of treatment, resulting in a biomass reduction of approximately 97 % (Fig. 2).

A time- and concentration-dependent effect was observed for *Ch*GH20 treatment (Fig. 2), with biomass reduction ranging from

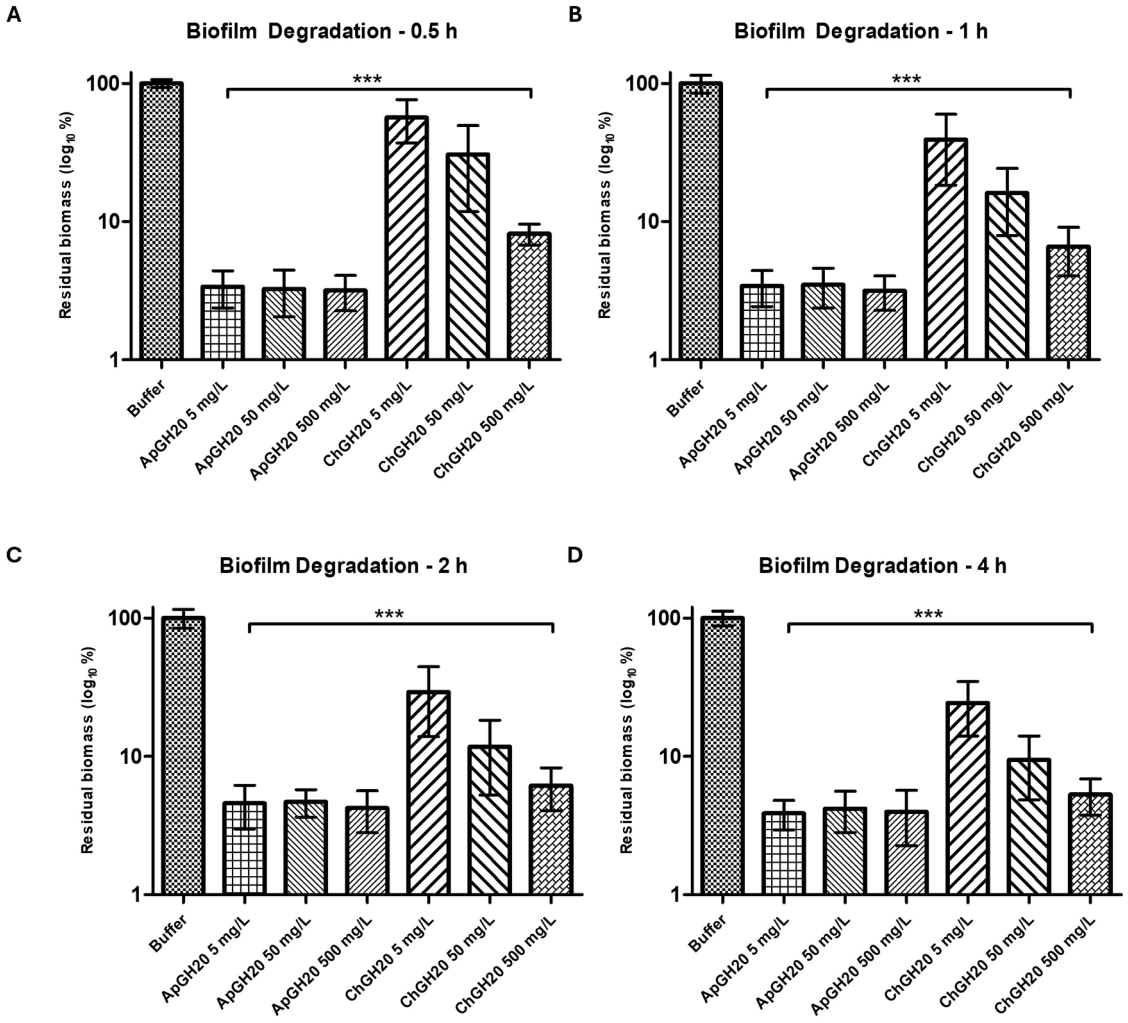

Fig. 2. Pre-formed *S. aureus 03* Biofilm Degradation by different *Ap*GH20 or *Ch*GH20 concentrations. A – 0.5 h treatment, B – 1 h treatment, C – 2 h treatment, D – 4 h treatment. Bars represent the standard deviation. *P*-value < 0.01; ns (nonsignificant difference) One-way ANOVA with Tukey's multiple comparisons test.

approximately 44 % (after 0.5 h of treatment with 5 mg/L *Ch*GH20) to nearly 95 % (after 4 h treatment with 500 mg/L *Ch*GH20) (Fig. 2). These results were confirmed by CLSM analysis of *S. aureus* 03 biofilm degradation (Fig. 3). The 3D reconstruction of the untreated *S. aureus* 03 controls revealed a robust biofilm, characterized by a thick carbohydrate–protein matrix (Calcofluor White/SYPRO Ruby staining) embedding viable cells (Syto 9 staining) (Fig. 3a). Both *Ap*GH20 and *Ch*GH20 treatments degraded all analyzed polymeric components (Fig. 3b&c); however, only *Ap*GH20 detached more residual viable cells, as also quantified by average fluorescence intensity (Fig. 3d).

When applied prior to the development of *S. aureus* 03 biofilm, both enzymes strongly reduced the amount of biofilm produced (Fig. 4). *Ap*GH20 yielded better results at lower enzyme concentrations as compared to *Ch*GH20.

Both enzymes, when used alone, were effective in preventing biofilm development as well as in degrading the existing extracellular matrix. Additionally, they enhanced the performance of gentamicin. Although gentamicin has a rapid bactericidal effect, this aminoglycoside is rarely used as monotherapy for treating *S. aureus* infections and is typically combined with a cell wall synthesis inhibitor. In fact, when applied to *S. aureus 03* biofilm, gentamicin was ineffective in killing bacterial cells, even at concentrations higher than 8 mg/L. However, pretreating the biofilm with either *Ap*GH20 or *Ch*GH20 for 1 h made it possible for gentamicin at 0.5 mg/L concentration to eliminate the remaining bacterial cells (Fig. 5), representing a >16-fold decrease in the required effective concentration.

In particular, the results shown in Fig. 5 demonstrate that pretreatment of biofilms with either *Ap*GH20 or *Ch*GH20 for 1 h led to undetectable metabolic activity of *S. aureus* upon subsequent exposure to gentamicin at 0.5 mg/L, a response indistinguishable from the sterility

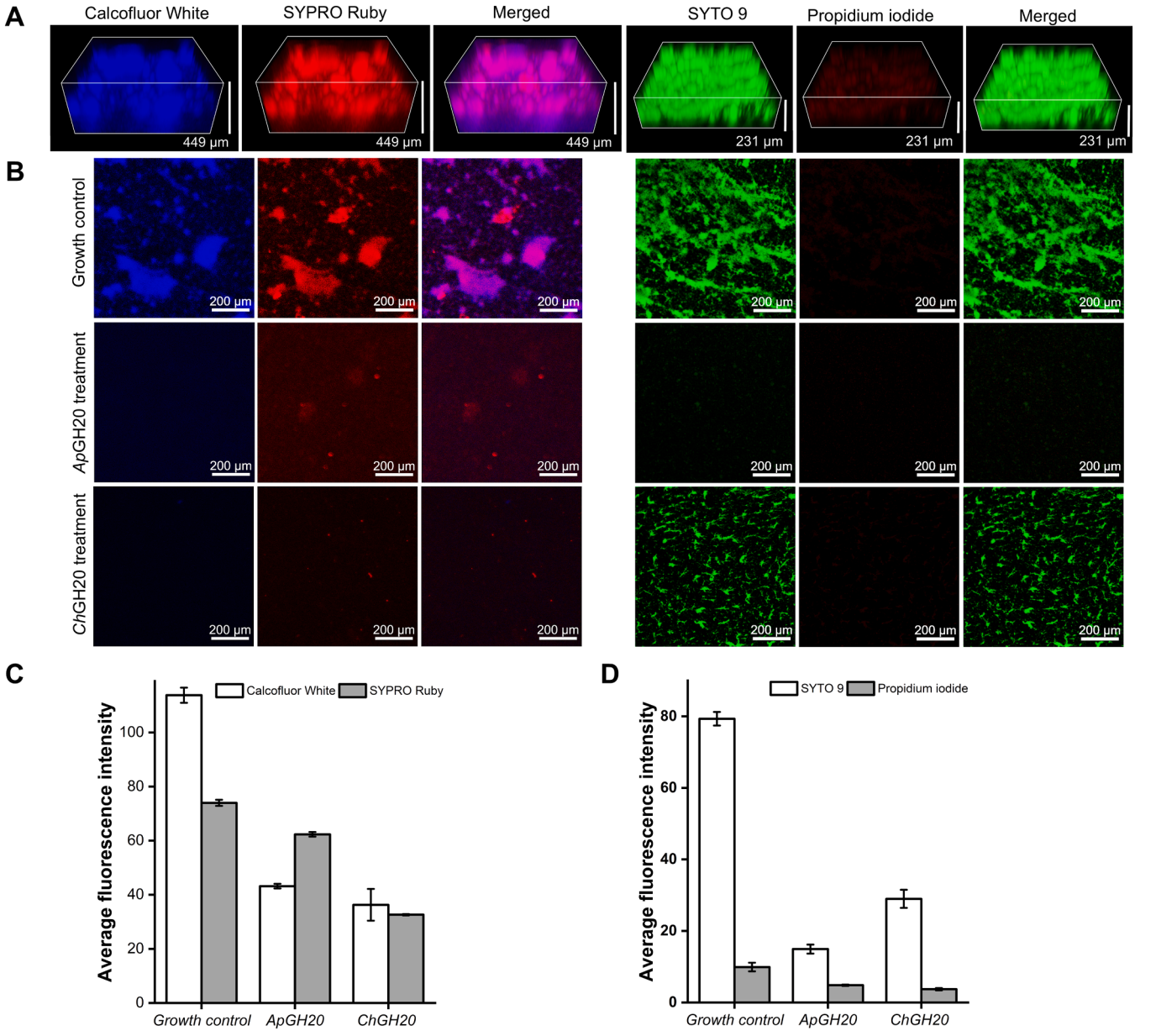

Fig. 3. Confocal laser scanning microscopy (CLSM) analysis of *S. aureus* 03 eradication. A – Three-dimensional CLSM image of *S. aureus* 03 biofilm growth controls, the protein matrix appears in red, while carbohydrates are visualized in blue after staining with SYPRO Ruby and Calcofluor White, respectively. Viable cells are detected in the green fluorescence channel, whereas dead cells are identified in the red fluorescence channel. B – CLSM analysis of *S. aureus* 03 biofilm degradation by *Ap*GH20 and *Ch*GH20. C – Arithmetic mean fluorescence intensity of the Calcofluor White/SYPRO Ruby double stain. D – Arithmetic mean fluorescence intensity of the LIVE/DEAD BacLight Bacterial Viability test (SYTO 9/propidium iodide).

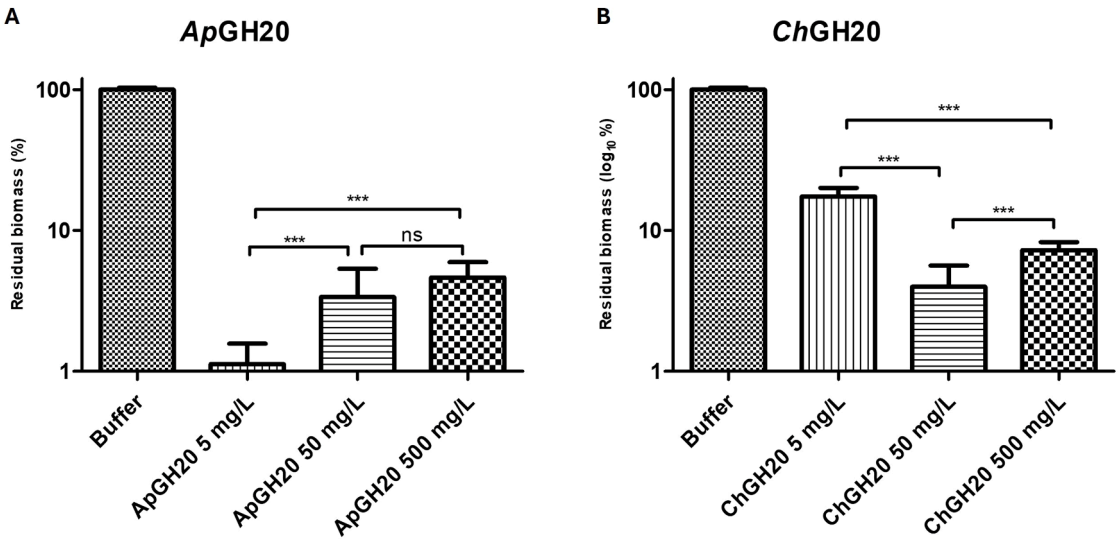

Fig. 4. Inhibition of *S. aureus 03* Biofilm Formation by different concentrations of enzymes. A – *Ap*GH20 treatment, B – *Ch*GH20 treatment. Bars represent the standard deviation. *P*-value < 0.01; ns (nonsignificant difference) One-way ANOVA with Tukey's multiple comparisons test.

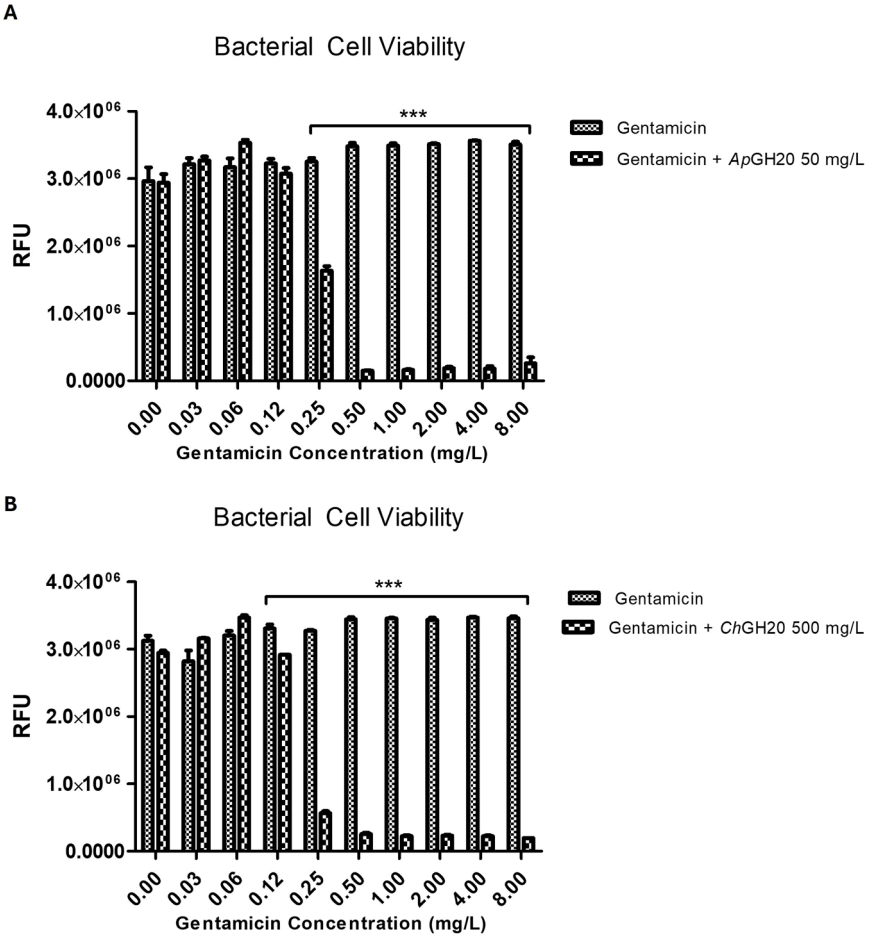

Fig. 5. Inhibitory activity of different concentrations of Gentamicin alone and after pre-treatment with A - 50 mg/L of *Ap*GH20, or B - 500 mg/L of *Ch*GH20 against *S. aureus* 03 biofilm. Values represent mean ± standard deviation of the mean (SEM) from three independent experiments. RFU – Relative Fluorescence Units. Two-way ANOVA revealed significant effects of concentration ($p < 0.0001$), treatment ($p < 0.0001$), and concentration × treatment interaction ($p = < 0.0001$). Bonferroni's post hoc test indicated greater bacterial inhibition for the combined treatment compared to Gentamicin alone starting from 0.25 mg/L for *Ap*GH20 and 0.125 mg/L for *Ch*GH20 (***$p < 0.001$).

controls. One-way ANOVA further revealed that enzymatic pretreatment significantly enhanced the activity of gentamicin against the tested *S. aureus* isolate at concentrations as low as 0.25 mg/L. In contrast, gentamicin alone, even at the highest concentration tested (8 mg/L), showed no measurable effect on metabolic activity (Fig. 5). These findings indicate that enzymatic pretreatment increased *S. aureus* susceptibility to gentamicin by at least 16-fold (from 8 mg/L down to 0.5 mg/L, a concentration statistically equivalent to the sterility control). Collectively, the data provide strong evidence that enzymatic biofilm disruption markedly potentiates gentamicin efficacy against the studied *S. aureus* strain.

3.4. Understanding the differences in the biofilm degradation capabilities of ApGH20 and ChGH20

To investigate the differences in biofilm degradation by *S. aureus* 03 between our enzymes, we conducted a dose-response experiment using lower concentrations than in previous assays to determine the half-maximal effective concentration (EC_{50}) for biofilm degradation. We found that the EC_{50} of *Ap*GH20 is approximately 141.6 pM, while that of *Ch*GH20 is 91.8 nM (Fig. 6a). This substantial difference of three orders of magnitude suggests that *Ap*GH20 is significantly more efficient in the *S. aureus* biofilm degradation (Fig. 5a).

Using structural alignment with Dispersin B and previous functional studies [33,34], we analyzed key determinants for PNAG recognition. One crucial aromatic residue, Tyr187 in DspB, has been reported as essential for PNAG recognition [34,35]. We identified this residue in both of the studied enzymes; however, it is displaced and positioned away from the catalytic residues (Fig. 6b). Furthermore, it does not adopt the protruding conformation observed in DspB. Another important determinant of the substrate binding is a set of anionic residues located in loops, such as Asp147, Asp245, and Glu248 in DspB [33]. Although *Ap*GH20 lacks these exact residues, it preserves the negatively charged cluster with Asp236 and Glu135. In contrast, *Ch*GH20 has these key anionic residues replaced by hydrophobic (Ile251) and positively charged (Arg151) amino acid residues, which is likely to reduce the enzyme ability to recognize and bind to PNAG.

We mapped all other anionic residues on Loops 1 and 3, highlighting those that are surface-exposed and may contribute to PNAG interaction (Fig. 6c, Supplementary Figure S4). In *Ap*GH20, Glu235 could enhance the electronegative environment alongside with Asp236. In contrast, *Ch*GH20 features Asp147, which may somewhat counterbalance the presence of Arg151, as it is oriented similarly to Asp127 in DspB and Glu135 in *Ap*GH20.

The acidic residues in Loops 1 and 3, when oriented toward the catalytic site, are essential for substrate recognition. Thus, the presence of Ile251 in Loop 3 could explain *Ch*GH20′s lower *S. aureus* biofilm degradation capacity. Asp248 might partially compensate for this effect, but this hypothesis needs to be tested with site-directed mutagenesis experiments.

3.5. Application and disruption of S. aureus biofilm from veterinary isolates

*Ap*GH20 and *Ch*GH20 degradation of biofilm-forming *S. aureus* isolates derived from bovine mastitis were investigated. Application of 50 mg/L of *Ap*GH20 or *Ch*GH20 to five different isolates resulted in partial degradation of MSA22 and MSA90 (Fig. 7a), with degradation levels

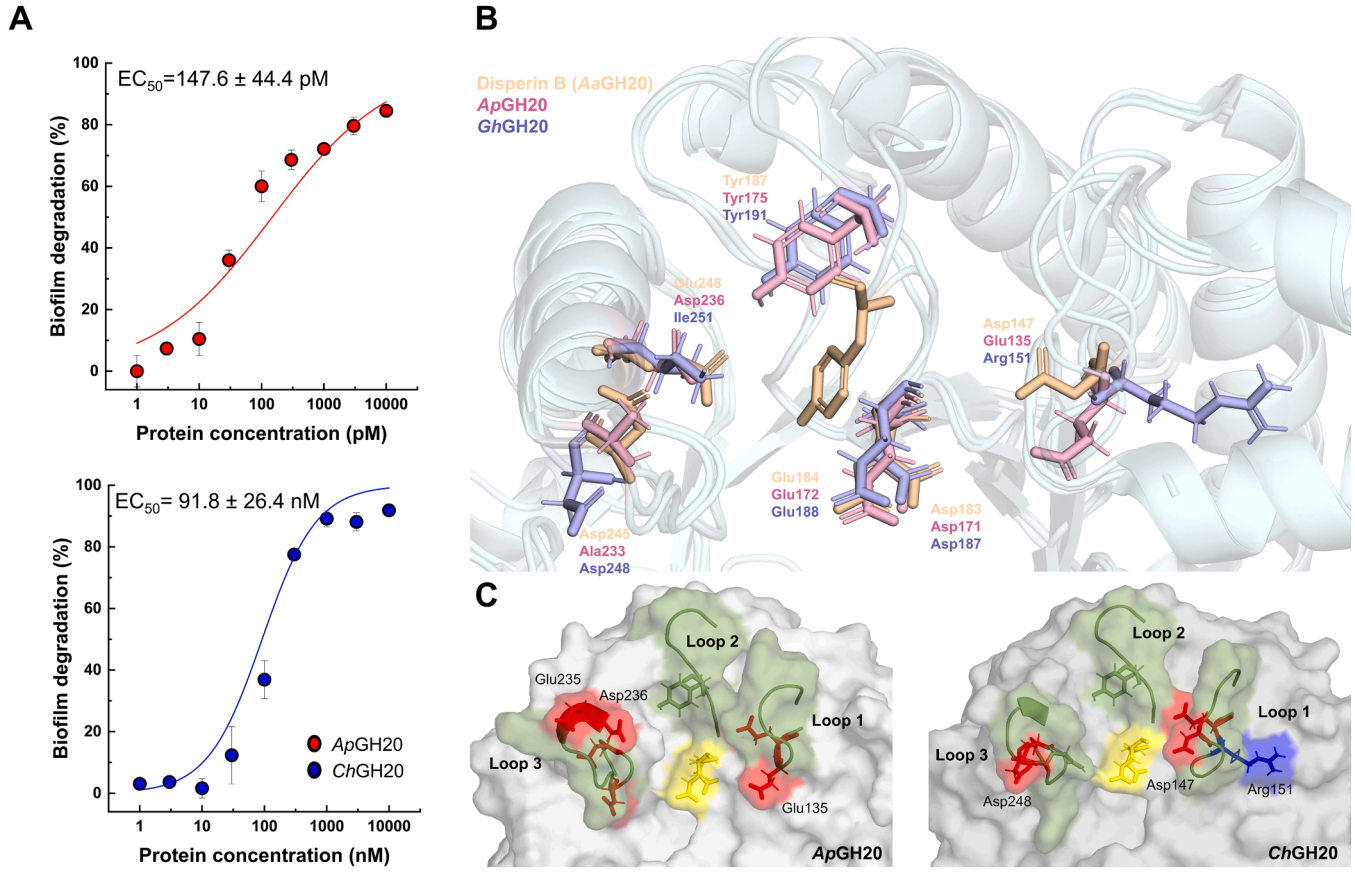

Fig. 6. Differential degradation of *S. aureus* 03 biofilms by *Ap*GH20 and *Ch*GH20. A - Dose-response experiments to determine the EC_{50} for the degradation of preformed biofilms. B-Structural alignment of the predicted models of *Ap*GH20 (pink) and *Ch*GH20 (blue) with DspB (yellow, PDB: 1YHT), highlighting key amino acids involved in PNAG binding as stick representations. C - Visualization of anionic residues (red sticks) within their corresponding loops (green cartoon representation), associated with substrate recognition and the catalytic site (yellow sticks).

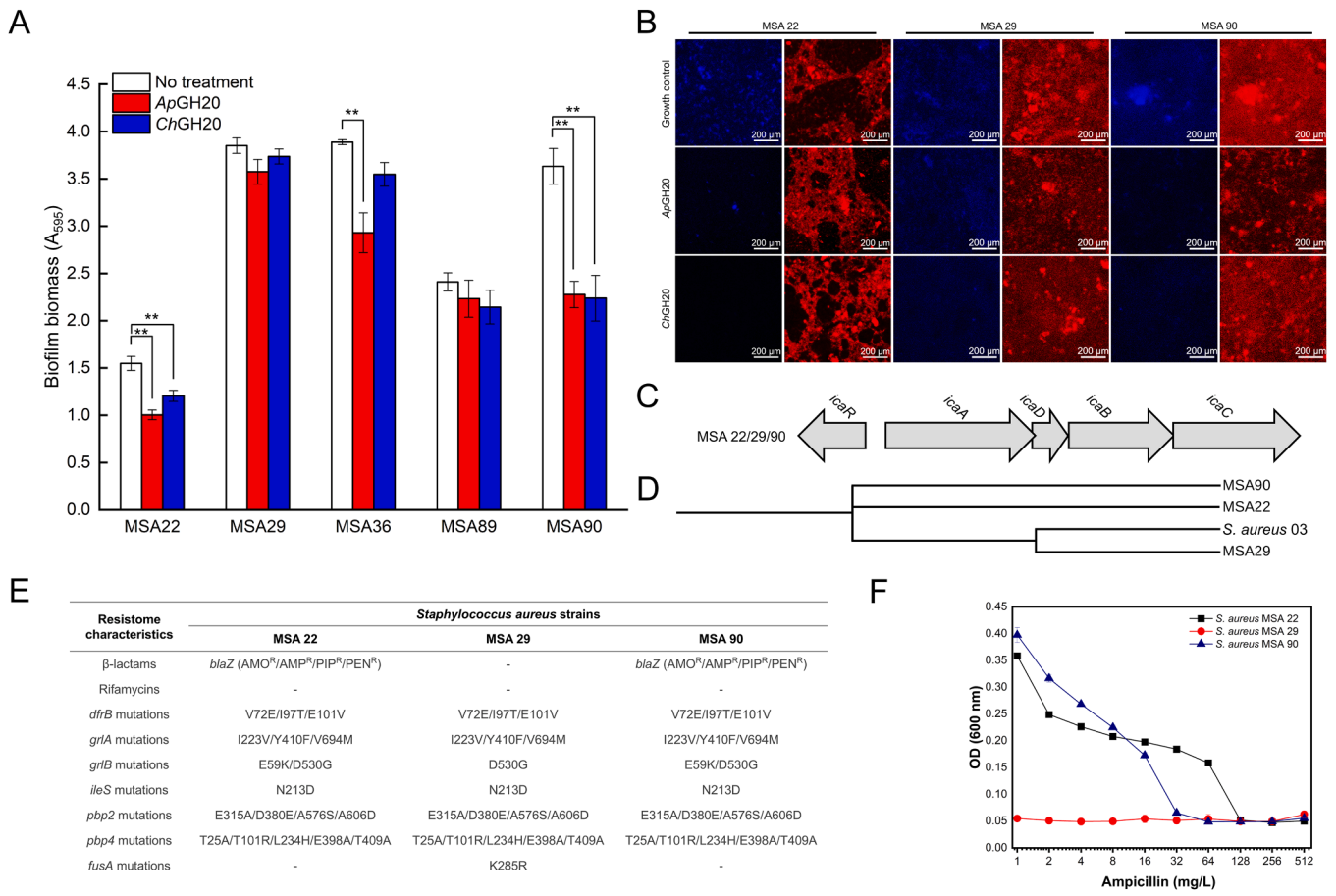

Resistome characteristics	*Staphylococcus aureus* strains		
	MSA 22	MSA 29	MSA 90
β-lactams	*blaZ* (AMO^R/AMP^R/PIP^R/PEN^R)	-	*blaZ* (AMO^R/AMP^R/PIP^R/PEN^R)
Rifamycins	-	-	-
dfrB mutations	V72E/I97T/E101V	V72E/I97T/E101V	V72E/I97T/E101V
grlA mutations	I223V/Y410F/V694M	I223V/Y410F/V694M	I223V/Y410F/V694M
grlB mutations	E59K/D530G	D530G	E59K/D530G
ileS mutations	N213D	N213D	N213D
pbp2 mutations	E315A/D380E/A576S/A606D	E315A/D380E/A576S/A606D	E315A/D380E/A576S/A606D
pbp4 mutations	T25A/T101R/L234H/E398A/T409A	T25A/T101R/L234H/E398A/T409A	T25A/T101R/L234H/E398A/T409A
fusA mutations	-	K285R	-

Fig. 7. Degradation of *S. aureus* biofilms associated with bovine mastitis. A - CV staining test for screening *S. aureus* biofilms susceptible to GH20 enzymatic treatment. B - CLSM analysis using Calcofluor White and SYPRO Ruby to assess the composition of selected veterinary biofilms and the effect of *Ap*GH20 and *Ch*GH20. C - Schematic of the *ica* operon obtained from the genome sequence analysis of MSA90, MSA29, and MSA22. D - Phylogenetic tree constructed using the sequenced genomes of veterinary isolates and *S. aureus* 03. E - ResFinder prediction of resistance genes and mutations. F - MIC test using ampicillin as the standard antibiotic. Bars represent the standard deviation. *P*-value < 0.01; ns (nonsignificant difference) One-way ANOVA with Tukey's multiple comparisons test.

ranging from 22 % to 38 %. Additionally, application of *Ap*GH20 lead to a 25 % degradation of MSA36.

Confocal laser scanning microscopy (CLSM) studies of representative biofilms (MSA90, MSA22, and MSA29) are in line with the observed degradation effects (Fig. 7b). The analysis also provided insights into biofilm composition, showing that the proteinaceous content exceeded the carbohydrate content. Hypothesized based on CLSM signal distribution, this imbalance may explain why the biofilms were not completely degraded.

Genome sequencing of these isolates revealed the presence of a complete *ica* operon (Fig. 7c). Furthermore, a phylogenetic tree based on genomic data (Fig. 7d) showed that MSA22 and MSA90 are the closest relatives, with only a slight genetic difference based on branch length. These two isolates formed biofilms that were susceptible to enzymatic treatments (Fig. 7a). In contrast, the non-susceptible MSA29 isolate has diverged from the previous two strains, while the human strain *S. aureus* 03 is the most distantly related, with a much longer branch length.

A preliminary analysis of the resistome of these veterinary isolates using the ResFinder database reveals that the MSA22 and MSA90 isolates also shares the *blaZ* gene, which confers resistance to β-lactams (Fig. 7e). This resistance was confirmed by ampicillin broth microdilution, with MSA22 exhibiting a MIC of 128 mg/L and MSA90 a MIC of 32 mg/L (Fig. 7f). While the correlation between biofilm formation and antibiotic resistance is well established in human isolates [36], it remains less clear in veterinary strains [37]. Further studies on these pathogens are necessary, as mastitis continues to be a significant disease burden in bovines [38]. We acknowledge that our hypothesis of the bacterial isolate biofilms more limited enzymatic response is based on our genome investigations and confocal microscopy data. It is important to emphasize, however, that these interpretations are not intended to establish enzyme specificity, but rather to provide a mechanistic rationale for the observed differences in biofilm degradation efficiency.

4. Discussion

4.1. Molecular characterization of S. aureus strains

Although *S. aureus* 03 is a methicillin-susceptible *S. aureus* (MSSA) strain, resistant to beta-lactams and rifampin, it is closely related to the USA300 clone (Supplementary Figure 5), a methicillin-resistant *S. aureus* (MRSA) strain of ST8 and t008, which is widespread in North America and associated with community-acquired infections [39]. Recently, this strain has also been reported in Brazilian hospitals [40–42].

Regarding the virulence genes found in the *S. aureus* 03 genome, the γ-hemolysin locus, present in nearly all *S. aureus* strains, consists of two S subunits (HlgA and HlgC) and one F subunit (HlgB), all encoded by the *hlgACB* locus. The HlgAB combination is capable of lysing both red blood cells and leukocytes, while HlgCB primarily exhibits leukotoxic activity. Although its precise role is not yet fully understood, it is believed that γ-hemolysin contributes to the blood proliferation of *S. aureus* by evading macrophages through lysis and capturing iron, released by lysed red blood cells. The leukotoxin LukED, like γ-hemolysin, exhibits activity against both leukocytes and red blood cells. It is a widespread

bicomponent pore-forming toxin, particularly common among community-acquired *S. aureus* strains. In addition to mediating cell lysis, LukED can induce the production of proinflammatory cytokines [43]. Aureolysin is a metalloprotease, while *splABCDEF* encode six serine-like proteases, all of which are secreted. Although the exact functions of these secreted proteases in *S. aureus* remain somewhat contradictory, recent studies suggest that their absence may lead to a hypervirulent phenotype. These proteases are thought to regulate virulence factors, controlling the severity and progression of disease, besides playing a role in cleaving host proteins, which aids in bacterial invasion [44,45].

Although most biofilm-producing *S. aureus* strains generate a PNAG-based extracellular matrix, some might produce a PNAG-independent biofilms, which contain proteins and extracellular DNA [46,47]. The complete *ica* operon was found in *S. aureus* 03 genome, however its *icaR* gene was truncated. IcaR, is a transcriptional regulator belonging to the TetR family, known to strongly repress the expression of the *ica* operon [48]. Thus, this mutation of the repressor is presumable responsible for the highly mucoid phenotype of *S. aureus* 03, producing abundant biofilm rich in PNAG [49].

4.2. Structural characterization of ApGH20 and ChGH20

The phylogenetic tree (Methods in Supplementary material) of the multi-activity GH20 family illustrates the extensive diversity of these enzymes (Supplementary Figure S6a). Notably, the only enzyme characterized using X-ray crystallography and extensively studied for its ability to degrade poly-β-1,6-N-acetyl-D-glucosamine oligomers is DspB [27]. Among the enzymes analyzed, *Ap*GH20 is most closely related to DspB, followed by *Ch*GH20. Within the same cluster, the catalytic modules A and B of StrH from *Streptococcus pneumoniae* are closely related to the latter enzymes. StrH specifically degrades terminal GlcNAc residues β-(1,2)-linked to mannose [50]. Another distinct cluster, which includes chitobiose hydrolase-like enzymes such as SpHEX, [51] further highlights the high diversity within the GH20 family.

Additionally, it is important to note that the primary structure of *Ch*GH20 exhibits a modular architecture, closely associated with adjacent domains (Supplementary Figure S6b). In contrast, *Ap*GH20 contains only a glycoside hydrolase domain in its structure.

The predicted three-dimensional structures of both enzymes reveal a $(\beta/\alpha)_8$ TIM barrel fold, with the catalytic site located at the center of the β-barrel (Supplementary Figure S6c). This site features an electronegative surface with a catalytic dyad [9]: Asp171/Glu172 for *Aa*GH20 and Asp187/Glu188 for *Ch*GH20 (Supplementary Figure S4, S6c).

4.3. Biological applications of ApGH20 and ChGH20

The strong PNAG-based biofilm production by *S. aureus* 03 facilitates the studies of *Ap*GH20 and *Ch*GH20 degradation of the pre-formed biofilm, which was accomplished with enzymes' concentrations as little as 5 mg/L. When Kaplan et. al (2003) first applied Dispersin B (50 mg/L) from *A. actinomycetemcomitans* to the biofilm of *S. aureus* strain for 6 hours, this resulted in approximately 85 % reduction in biomass [8]. The following year, the same authors tested the performance of Dispersin B from *A. actinomycetemcomitans* on *Staphylococcus epidermidis* biofilms, reporting that a 30-minute treatment using 40 mg/L of the enzyme left virtually undetectable biofilms [10]. These findings indicate that other Dispersin B orthologs can be effective against PNAG-based bacterial biofilms.

*Ap*GH20 and *Ch*GH20 were also effective in inhibiting the formation of biofilm by *S. aureus* 03. Similarly, Yu et al. demonstrated that the glycoside hydrolase PslG from *P. aeruginosa* not only prevented biofilm formation but also disrupted pre-existing *P. aeruginosa* biofilms, [7] highlighting that this is a common feature among biofilm-active glycoside hydrolases.

Together, these findings strongly support the conclusion that both *Ap*GH20 and *Ch*GH20 are active against *S. aureus* biofilms. The enzymes not only hydrolyze the synthetic substrate pNP-β-*N*-acetylglucosamine, but also effectively degrade PNAG-dependent biofilms. Their activity is particularly pronounced against the *S. aureus* 03 strain, which carries a mutation in the *icaR* repressor leading to uncontrolled synthesis of PNAG-rich biofilms. Importantly, no comparable effect was observed with the enzyme-free buffer control, while confocal microscopy further confirmed the efficient disruption of *S. aureus* biofilms by both enzymes.

When pre-treating the *S. aureus* 03 biofilm with *Ap*GH20 or *Ch*GH20 prior to gentamicin treatment, the efficiency of this antimicrobial could be enhanced. Our hypothesis is that the enzymatic degradation of the main component of the extracellular polymeric matrix renders the biofilm-embedded bacterial cells more accessible, more similar to their planktonic counterparts, thereby facilitating an access of the gentamicin to the bacterial cells. Binding of irreversible inhibitor of bacterial protein synthesis, gentamicin, to the 30S ribosomal subunit of the bacterial ribosome disrupts the normal translation process, ultimately leading to bacterial cell death. We speculate that the antibiotic's effectiveness is improved by enzymatic degradation of *S. aureus* biofilms is due to its enhanced ability to reach and to penetrate the bacterial cell membrane, thus allowing it to more efficiently exert its bactericidal effects. Similar results were recently reported by Kaplan et al. with *Cutibacterium acnes*, the causative agent of acne vulgaris [52]. They first confirmed that biofilms of this species contained PNAG and then demonstrated that the presence of Dispersin B from *A. actinomycetemcomitans* reduced tetracycline tolerance in the biofilms [52].This effect is not limited to Dispersin B-like enzymes. For instance, a study combining an enzyme cocktail (comprising an endo-1,4-β-D-glucanase, a β-1,6-hexosaminidase, and an RNA/DNA nonspecific endonuclease) with several antibiotics, showed a synergistic effect on biofilms of *S. aureus, S. epidermidis*, and *E. coli* in prosthetic joint models [53]. Similarly, a combination of cellulase and ceftazidime reduced the Minimum Biofilm Eradication Concentration (MBEC) of *P. aeruginosa* biofilms by 32 to 128-fold [54]. Thus, enzymatic biofilm degradation could represent important addition to antibiotic therapy. Despite tremendous efforts to discover new active molecules, bacteria can quickly develop resistance shortly after these antibiotics are introduced to the market, limiting investments in antibiotic development [55,56]. Therefore, a viable solution for treating infections in biofilm-forming sites that are resistant to antibiotics could be the combination of enzymes and antibiotics to improve their efficiency.

5. Conclusions

Given the limited efficacy of most antimicrobials in treating infections caused by bacterial biofilms, the use of glycoside hydrolases offers a promising alternative to improve their efficacy. This is particularly critical in the current landscape, characterized by insufficient investment in the development of new antimicrobial agents.

Both glycoside hydrolases studied here were effective in inhibiting the formation of biofilms by a *S. aureus* strain isolated from a human infection and in degrading of preformed biofilms of both human and veterinary *S. aureus* isolates. As expected, this effect was observed only in biofilms primarily composed of polysaccharides, but not proteins, as confirmed by CLSM and genomic analysis of the *ica* operon in the relevant strains. This specificity is a key feature of the enzymes and underscores the importance of selecting the appropriate enzyme for degrading biofilms, depending on their composition and the bacterial species or strain involved.

Following arguments support a notion that both investigated enzymes, ApGH20 and ChGH20, have activity against *S. aureus* biofilms: 1. ApGH20 and ChGH20 are enzymatically active against synthetic pNP-β-N-acetylglucosamine substrate; 2. the enzymes degrades PNAG-dependent *S. aureus* biofilms, 3. ApGH20 and ChGH20 are particularly efficient against S. aureus 03 strain which has a mutation in the icaR repressor, leading to unrestraint synthesis of PNAG-rich biofilms, 4. heat-treated enzymes and "no-enzyme" buffer were incapable of

S. aureus biofilm degradation (negative control), whereas 5. recombinant E. coli EcPgaB was efficient in *S. aureus* 03 biofilm degradation (positive control). Finally, 6. our confocal microscopy studies clearly demonstrate efficient degradation of *S. aureus* biofilms using both studied enzymes.

Furthermore, results shown in Fig. 5 clearly show that the biofilms pretreatment either with ApGH20 or ChGH20 for 1 hour result in undetectable metabolic activity of *S. aureus* after application of gentamicin at 0.5 mg/L concentration, which was undistinguishable from sterility control. Moreover, one-way ANOVA analysis shows that the enzymatic treatments have statistically relevant impacts on the gentamicin efficiency against studied *S. aureus* isolate at 0.25mg/L or less. At the same time the highest applied concentration of gentamicin alone (8mg/L) had no effect on the metabolic activity of the cells (Fig. 5). In fact, even much higher concentrations of the antibiotic (up to 100mg/L) were inefficient against *S. aureus* 03. This means that enzymatic treatment resulted in at least 16-fold increase in susceptibility of S. aureus cells to gentamicin after the enzymatic treatment (from 8mg/L down to 0.5mg/L, concentration which was statistically indistinguishable from the sterility control). In reality, the effect is probably much higher. Results presented in Fig. 5 leave no doubt that the gentamicin efficiency against studied *S. aureus* strain was indeed strongly boosted by the biofilm enzymatic degradation.

It is well established that infections caused by biofilms, whether in humans or animals, are often multi-species. This factor should be considered in future investigations, which may require the use of enzymatic cocktails to effectively target real-world biofilms.

The findings of this study highlight an alternative approach for treating *S. aureus* biofilm caused infections. Notably, even though complete sterilization has not been proven, strongly improved efficacy of gentamicin, when applied together with enzymatic treatment, could revive interest in this antimicrobial agent, which is seldom used alone for treatment of such infections. Gentamicin has the advantage of being easily produced, with its mechanism of action and toxicity well understood.

The establishment of effective technologies for applied settings will require extensive studies on novel enzymes capable of degrading the exopolysaccharide matrix of *S. aureus* biofilms, particularly GH20 glycoside hydrolases. While the discovery of Dispersin B represented a significant milestone, the large number of orthologs identified through recent genomic studies provides a promising foundation for future advances in this field. Continued investigation of PNAG-active enzymes, including those within the GH20 family, will be essential for the development of novel enzymatic catalysts with potential application in the degradation of PNAG-rich *S. aureus* biofilms.

It is important to acknowledge the limitations of current study. All results were obtained from *in vitro* experiments, and further *in vivo* validation is essential to confirm both the efficacy of the combined action of GH20 glycoside hydrolases and antibiotics, as well as the absence of toxicity. It should also be noted that these enzymes are more effective against biofilms formed by strains producing PNAG-rich extracellular polymeric substance, which may not be the case for all *S. aureus* strains. Furthermore, our study focuses solely on *in vitro* monoculture models and does not evaluate polymicrobial biofilms. While further research is needed to identify the optimal combinations of enzymes and antimicrobials for specific cases, the current efforts are highly valuable in light of the ongoing challenges posed by infectious diseases.

CRediT authorship contribution statement

Andrei Nicoli Gebieluca Dabul: Writing – review & editing, Writing – original draft, Methodology, Investigation, Formal analysis, Data curation, Conceptualization. **Lorgio Victor Bautista Samaniego:** Writing – original draft, Methodology, Investigation, Formal analysis, Data curation. **Anelyse Abreu Cortez:** Methodology, Investigation. **Samuel Luis Scandelau:** Methodology, Investigation, Formal analysis. **Marcelo Vizoná Liberato:** Methodology, Formal analysis. **Agatha MS Kubo:** Investigation, Formal analysis. **Ana Beatriz Rodrigues:** Investigation, Formal analysis. **Rejane MT Grotto:** Funding acquisition. **Guilherme Valente:** Supervision, Investigation, Formal analysis. **Vera Lúcia Mores Rall:** Resources, Conceptualization. **Sebastião Pratavieira:** Methodology, Investigation. **Mario de Oliveira Neto:** Project administration, Funding acquisition. **Carla Raquel Fontana:** Visualization, Supervision, Formal analysis. **Igor Polikarpov:** Writing – review & editing, Writing – original draft, Visualization, Supervision, Resources, Project administration, Funding acquisition, Formal analysis, Conceptualization.

Declaration of competing interest

The authors declare that they have no known competing financial interests or personal relationships that could have appeared to influence the work reported in this paper.

Acknowledgements

This work was supported by Conselho Nacional de Desenvolvimento Científico e Tecnológico (CNPq, grants # 306852/2021-7, 312025/2022-0 and 440180/2022-8) and the Fundação de Amparo à Pesquisa do Estado de São Paulo (FAPESP, grants # 2021/08780-1, 2024/00533-3, and 2022/02261-5) and by Brazilian Federal Deputy Tiririca.

Supplementary materials

Supplementary material associated with this article can be found, in the online version, at doi:10.1016/j.actbio.2025.10.032.

References

[1] K.S. Ikuta, L.R. Swetschinski, G.R. Aguilar, F. Sharara, T. Mestrovic, A.P. Gray, N. D. Weaver, E.E. Wool, C. Han, A.G. Hayoon, A. Aali, S.M. Abate, M. Abbasi-Kangevari, Z. Abbasi-Kangevari, S. Abd-Elsalam, G. Abebe, A. Abedi, A.P. Abhari, H. Abidi, R.G. Aboagye, A. Absalan, H.A. Ali, J.M. Acuna, T.D. Adane, I.Y. Addo, O. A. Adegboye, M. Adnan, Q.E.S. Adnani, M.S. Afzal, S. Afzal, Z.B. Aghdam, B. O. Ahinkorah, A. Ahmad, A.R. Ahmad, R. Ahmad, S. Ahmad, S. Ahmad, S. Ahmadi, A. Ahmed, H. Ahmed, J.Q. Ahmed, T.A. Rashid, M. Ajami, B. Aji, M. Akbarzadeh-Khiavi, C.J. Akunna, H. Al Hamad, F. Alahdab, Z. Al-Aly, M.A. Aldeyab, A. V. Aleman, F.A.N. Alhalaiqa, R.K. Alhassan, B.A. Ali, L. Ali, S.S. Ali, Y. Alimohamadi, V. Alipour, A. Alizadeh, S.M. Aljunid, K. Allel, S. Almustanyir, E. K. Ameyaw, A.M.L. Amit, N. Anandavelane, R. Ancuceanu, C.L. Andrei, T. Andrei, D. Anggraini, A. Ansar, A.E. Anyasodor, J. Arabloo, A.Y. Aravkin, D. Areda, T. Aripov, A.A. Artamonov, J. Arulappan, R.T. Aruleba, M. Asaduzzaman, T. Ashraf, S.S. Athari, D. Atlaw, S. Attia, M. Ausloos, T. Awoke, B.P.A. Quintanilla, T.M. Ayana, S. Azadnajafabad, A.A. Jafari, B. Darshan, M. Badar, A.D. Badiye, N. Baghcheghi, S. Bagherieh, A.A. Baig, I. Banerjee, A. Barac, M. Bardhan, F. Barone-Adesi, H.J. Barqawi, A. Barrow, P. Baskaran, S. Basu, A.M.M. Batiha, N. Bedi, M.A. Belete, U.I. Belgaumi, R.G. Bender, B. Bhandari, D. Bhandari, P. Bhardwaj, S. Bhaskar, K. Bhattacharyya, S. Bhattarai, S. Bitaraf, D. Buonsenso, Z. A. Butt, F.L.C.Dos Santos, J. Cai, D. Calina, P. Camargos, L.A. Cámera, R. Cárdenas, M. Cevik, J. Chadwick, J. Charan, A. Chaurasia, P.R. Ching, S.G. Choudhari, E. K. Chowdhury, F.R. Chowdhury, D.T. Chu, I.S. Chukwu, O. Dadras, F.T. Dagnaw, X. Dai, S. Das, A. Dastiridou, S.A. Debela, F.W. Demisse, S. Demissie, D. Dereje, M. Derese, H.D. Desai, F.N. Dessalegn, S.A.A. Dessalegni, B. Desye, K. Dhaduk, M. Dhimal, S. Dhingra, N. Diao, D. Diaz, S. Djalalinia, M. Dodangeh, D. Dongarwar, B.T. Dora, F. Dorostkar, H.L. Dsouza, E. Dubljanin, S.J. Dunachie, O.C. Durojaiye, H.A. Edinur, H.B. Ejigu, M. Ekholuenetale, T.C. Ekundayo, H. El-Abid, M. Elhadi, M.A. Elmonem, A. Emami, L.E. Bain, D.B. Enyew, R. Erkhembayar, B. Eshrati, F. Etaee, A.F. Fagbamigbe, S. Falahi, A. Fallahzadeh, E.J.A. Faraon, A. Fatehizadeh, G. Fekadu, J.C. Fernandes, A. Ferrari, G. Fetensa, I. Filip, F. Fischer, M. Foroutan, P. A. Gaal, M.A. Gadanya, A.M. Gaidhane, B. Ganesan, M. Gebrehiwot, R. Ghanbari, M.G. Nour, A. Ghashghaee, A. Gholamrezanezhad, A. Gholizadeh, M. Golechha, P. Goleij, D. Golinelli, A. Goodridge, D.A. Gunawardane, Y. Guo, R.Das Gupta, S. Gupta, V.B. Gupta, V.K. Gupta, A. Guta, P. Habibzadeh, A.H. Avval, R. Halwani, A. Hanif, M.A. Hannan, H. Harapan, S. Hassan, H. Hassankhani, K. Hayat, B. Heibati, G. Heidari, M. Heidari, R. Heidari-Soureshjani, C. Herteliu, D.Z. Heyi, K. Hezam, P. Hoogar, N. Horita, M.M. Hossain, M. Hosseinzadeh, M. Hostiuc, S. Hostiuc, S. Hoveidamanesh, J. Huang, S. Hussain, N.R. Hussein, S.E. Ibitoye, O. S. Ilesanmi, I.M. Ilic, M.D. Ilic, M.T. Imam, M. Immurana, L.R. Inbaraj, A. Iradukunda, N.E. Ismail, C.C.D. Iwu, C.J. Iwu, M.J. Linda, M. Jakovljevic, E. Jamshidi, T. Javaheri, F. Javanmardi, J. Javidnia, S.K. Jayapal, U. Jayarajah, R. Jebai, R.P. Jha, T. Joo, N. Joseph, F. Joukar, J.J. Jozwiak, S.E.O. Kacimi, V. Kadashetti, L.R. Kalankesh, R. Kalhor, V.K. Kamal, H. Kandel, N. Kapoor,

S. Karkhah, B.G. Kassa, N.J. Kassebaum, P.D.M.C. Katoto, M. Keykhaei, H. Khajuria, A. Khan, I.A. Khan, M. Khan, M.N. Khan, M.A.B. Khan, M. M. Khatatbeh, M.M. Khater, H.R.K. Kashani, J. Khubchandani, H. Kim, M.S. Kim, R. W. Kimokoti, N. Kissoon, S. Kochhar, F. Kompani, S. Kosen, P.A. Koul, S.L. K. Laxminarayana, F.K. Lopez, K. Krishan, V. Krishnamoorthy, V. Kulkarni, N. Kumar, O.P. Kurmi, A. Kuttikkattu, H.H. Kyu, D.K. Lal, J. Lám, I. Landires, S. Lasrado, S.W. Lee, J. Lenzi, S. Lewycka, S. Li, S.S. Lim, W. Liu, R. Lodha, M. J. Loftus, A. Lohiya, L. Lorenzovici, M. Lotfi, A. Mahmoodpoor, M.A. Mahmoud, R. Mahmoudi, A. Majeed, J. Majidpoor, A. Makki, G.A. Mamo, Y. Manla, M. Martorell, C.N. Matei, B. Mcmanigal, E.M. Nasab, R. Mehrotra, A. Melese, O. Mendoza-Cano, R.G. Menezes, A.F.A. Mentis, G. Micha, I.M. Michalek, A.C.M.G. N. Des, N.M. Kostova, S.A. Mir, M. Mirghafourvand, S. Mirmoeeni, E. M. Mirrakhimov, M. Mirza-Aghazadeh-attari, A.S. Misganaw, A. Misganaw, S. Misra, E. Mohammadi, M. Mohammadi, A. Mohammadian-Hafshejani, S. Mohammed, S. Mohan, M. Mohseni, A.H. Mokdad, S. Momtazmanesh, L. Monasta, C.E. Moore, M. Moradi, M.M. Sarabi, S.D. Morrison, M. Motaghinejad, H.M. Isfahani, A.M. Khaneghah, S.A. Mousavi-Aghdas, S. Mubarik, F. Mulita, G.B. B. Mulu, S.B. Munro, S. Muthupandian, T.S. Nair, A.A. Naqvi, H. Narang, Z. S. Natto, M. Naveed, B.P. Nayak, S. Naz, I. Negoi, S.A. Nejadghaderi, S.N. Kandel, C.H. Ngwa, R.K. Niazi, A.T.N. Des, N. Noroozi, H. Nouraei, A. Nowroozi, V. Nuñez-Samudio, J.J. Nutor, C.I. Nzoputam, O.J. Nzoputam, B. Oancea, R.M. Obaidur, V. A. Ojha, A.P. Okekunle, O.C. Okonji, A.T. Olagunju, B.O. Olusanya, A.O. Bali, E. Omer, N. Otstavnov, B. Oumer, J.R. Padubidri, K. Pakshir, T. Palicz, A. Pana, S. Pardhan, J.L. Paredes, U. Parekh, E.C. Park, S. Park, A. Pathak, R. Paudel, U. Paudel, S. Pawar, H.P. Toroudi, M. Peng, U. Pensato, V.C.F. Pepito, M. Pereira, M.F.P. Peres, N. Perico, I.R. Petcu, Z.Z. Piracha, I. Podder, N. Pokhrel, R. Poluru, M. J. Postma, N. Pourtaheri, A. Prashant, I. Qattea, M. Rabiee, N. Rabiee, A. Radfar, S. Raeghi, S. Rafiei, P.R. Raghav, L. Rahbarnia, V. Rahimi-Movaghar, M. Rahman, M.A. Rahman, A.M. Rahmani, V. Rahmanian, P. Ram, M.M.A.N. Ranjha, S.J. Rao, M.M. Rashidi, A. Rasul, Z.A. Ratan, S. Rawaf, R. Rawassizadeh, M.S. Razeghinia, E. M.M. Redwan, M.T. Regasa, G. Remuzzi, M.A. Reta, N. Rezaei, A. Rezapour, A. Riad, R.K. Ripon, K.E. Rudd, B. Saddik, S. Sadeghian, U. Saeed, M. Safaei, A. Safary, S.Z. Safi, M. Sahebazzamani, A. Sahebkar, H. Sahoo, S. Salahi, S. Salahi, H. Salari, S. Salehi, H.S. Kafil, A.M. Samy, N. Sanadgol, S. Sankararaman, F. Sanmarchi, B. Sathian, M. Sawhney, G.K. Saya, S. Senthilkumaran, A. Seylani, P. A. Shah, M.A. Shaikh, E. Shaker, M.Z. Shakhmardanov, M.M. Sharew, A. Sharifi-Razavi, P. Sharma, R.A. Sheikhi, A. Sheikhy, P.H. Shetty, M. Shigematsu, J.ll Shin, H. Shirzad-Aski, K.M. Shivakumar, P. Shobeiri, S.A. Shorofi, S. Shrestha, M. M. Sibhat, N.B. Sidemo, M.K. Sikder, L.M.L.R. Silva, J.A. Singh, P. Singh, S. Singh, M.S. Siraj, S.S. Siwal, V.Y. Skryabin, A.A. Skryabina, B. Socea, D.D. Solomon, Y. Song, C.T. Sreeramareddy, M. Suleman, R.S. Abdulkader, S. Sultana, M. Szócska, S.A. Tabatabaeizadeh, M. Tabish, M. Taheri, E. Taki, K.K. Tan, S. Tandukar, N. Y. Tat, V.Y. Tat, B.N. Tefera, Y.M. Tefera, G. Temesgen, M.H. Temsah, S. Tharwat, A. Thiyagarajan, I.I. Tleyjeh, C.E. Troeger, K.K. Umapathi, E. Upadhyay, S. V. Tahbaz, P.R. Valdez, J.Van Den Eynde, H.R. Van Doorn, S. Vaziri, G.I. Verras, H. Viswanathan, B. Vo, A. Waris, G.T. Wassie, N.D. Wickramasinghe, S. Yaghoubi, G.A.T.Y. Yahya, S.H.Y. Jabbari, A. Yigit, V. Yigit, D.K. Yon, N. Yonemoto, M. Zahir, B.A. Zaman, S.Bin Zaman, M. Zangiabadian, I. Zare, M.S. Zastrozhin, Z.J. Zhang, P. Zheng, C. Zhong, M. Zoladl, A. Zumla, S.I. Hay, C. Dolecek, B. Sartorius, C.J. L. Murray, M. Naghavi, Global mortality associated with 33 bacterial pathogens in 2019: a systematic analysis for the Global Burden of Disease Study 2019, Lancet 400 (2022) 2221–2248, https://doi.org/10.1016/S0140-6736(22)02185-7.

[2] G.Y.C. Cheung, J.S. Bae, M. Otto, Pathogenicity and virulence of Staphylococcus aureus, Virulence 12 (2021) 547–569, https://doi.org/10.1080/21505594.2021.1878688.

[3] P. François, J. Schrenzel, F. Götz, Biology and regulation of staphylococcal biofilm, Int. J. Mol. Sci. 24 (2023), https://doi.org/10.3390/IJMS24065218.

[4] J.B. Kaplan, K. Velliyagounder, C. Ragunath, H. Rohde, D. Mack, J.K.M. Knobloch, N. Ramasubbu, Genes involved in the synthesis and degradation of matrix polysaccharide in Actinobacillus actinomycetemcomitans and Actinobacillus pleuropneumoniae biofilms, J. Bacteriol. 186 (2004) 8213–8220, https://doi.org/10.1128/JB.186.24.8213-8220.2004.

[5] W.K. Redman, G.S. Welch, K.P. Rumbaugh, Differential efficacy of glycoside hydrolases to disperse biofilms, Front. Cell Infect. Microbiol. 10 (2020) 379, https://doi.org/10.3389/FCIMB.2020.00379/BIBTEX.

[6] F. Le Mauff, N.C. Bamford, N. Alnabelseya, Y. Zhang, P. Baker, H. Robinson, J.D. C. Codée, P.Lynne Howell, D.C. Sheppard, Molecular mechanism of Aspergillus fumigatus biofilm disruption by fungal and bacterial glycoside hydrolases, J. Biol. Chem. 294 (2019) 10760–10772, https://doi.org/10.1074/JBC.RA119.008511.

[7] S. Yu, T. Su, H. Wu, S. Liu, D. Wang, T. Zhao, Z. Jin, W. Du, M.J. Zhu, S.L. Chua, L. Yang, D. Zhu, L. Gu, L.Z. Ma, PslG, a self-produced glycosyl hydrolase, triggers biofilm disassembly by disrupting exopolysaccharide matrix, Cell Res. 25 (2015) 1352–1367, https://doi.org/10.1038/CR.2015.129.

[8] J.B. Kaplan, C. Ragunath, N. Ramasubbu, D.H. Fine, Detachment of Actinobacillus actinomycetemcomitans biofilm cells by an endogenous β-hexosaminidase activity, J. Bacteriol. 185 (2003) 4693–4698, https://doi.org/10.1128/JB.185.16.4693-4698.2003.

[9] J.B. Kaplan, S.A. Sukhishvili, M. Sailer, K. Kridin, N. Ramasubbu, Aggregatibacter actinomycetemcomitans Dispersin B: the quintessential antibiofilm enzyme, Pathogens 13 (2024), https://doi.org/10.3390/PATHOGENS13080668.

[10] J.B. Kaplan, C. Ragunath, K. Velliyagounder, D.H. Fine, N. Ramasubbu, Enzymatic detachment of Staphylococcus epidermidis biofilms, Antimicrob. Agents Chemother 48 (2004) 2633, https://doi.org/10.1128/AAC.48.7.2633-2636.2004.

[11] G. Procop, D. Church, G. Hall, W. Janda, E. Koneman, P. Schreckenberger, G. Woods, Koneman's color atlas and textbook of diagnostic microbiology, 7th ed, Jones & Bartlett Learning, Burlington, 2020.

[12] A.M. Bolger, M. Lohse, B. Usadel, Trimmomatic: A flexible trimmer for Illumina sequence data, Bioinformatics 30 (2014) 2114–2120, https://doi.org/10.1093/BIOINFORMATICS/BTU170.

[13] R.R. Wick, L.M. Judd, C.L. Gorrie, K.E. Holt, Unicycler: Resolving bacterial genome assemblies from short and long sequencing reads, PLoS Comput. Biol. 13 (2017), https://doi.org/10.1371/journal.pcbi.1005595.

[14] M. Alonge, L. Lebeigle, M. Kirsche, K. Jenike, S. Ou, S. Aganezov, X. Wang, Z. B. Lippman, M.C. Schatz, S. Soyk, Automated assembly scaffolding using RagTag elevates a new tomato system for high-throughput genome editing, Genome Biol. 23 (2022) 1–19, https://doi.org/10.1186/S13059-022-02823-7/FIGURES/2.

[15] R.K. Aziz, D. Bartels, A. Best, M. DeJongh, T. Disz, R.A. Edwards, K. Formsma, S. Gerdes, E.M. Glass, M. Kubal, F. Meyer, G.J. Olsen, R. Olson, A.L. Osterman, R. A. Overbeek, L.K. McNeil, D. Paarmann, T. Paczian, B. Parrello, G.D. Pusch, C. Reich, R. Stevens, O. Vassieva, V. Vonstein, A. Wilke, O. Zagnitko, The RAST server: rapid annotations using subsystems technology, BMC Genom. 9 (2008) 1–15, https://doi.org/10.1186/1471-2164-9-75/TABLES/3.

[16] B.P. Alcock, W. Huynh, R. Chalil, K.W. Smith, A.R. Raphenya, M.A. Wlodarski, A. Edalatmand, A. Petkau, S.A. Syed, K.K. Tsang, S.J.C. Baker, M. Dave, M. C. Mccarthy, K.M. Mukiri, J.A. Nasir, B. Golbon, H. Imtiaz, X. Jiang, K. Kaur, M. Kwong, Z.C. Liang, K.C. Niu, P. Shan, J.Y.J. Yang, K.L. Gray, G.R. Hoad, B. Jia, T. Bhando, L.A. Carfrae, M.A. Farha, S. French, R. Gordzevich, K. Rachwalski, M. M. Tu, E. Bordeleau, D. Dooley, E. Griffiths, H.L. Zubyk, E.D. Brown, F. Maguire, R. G. Beiko, W.W.L. Hsiao, F.S.L. Brinkman, G. Van Domselaar, A.G. Mcarthur, CARD 2023: expanded curation, support for machine learning, and resistome prediction at the Comprehensive Antibiotic Resistance Database, Nucleic. Acids. Res. 51 (2023) D690–D699, https://doi.org/10.1093/NAR/GKAC920.

[17] Clinical Laboratory Standards Institute, M100 Performance Standards for Antimicrobial Susceptibility Testing, Wayne, PA, 2020.

[18] F. Bertels, O.K. Silander, M. Pachkov, P.B. Rainey, E. Van Nimwegen, Automated reconstruction of whole-genome phylogenies from short-sequence reads, Mol. Biol. Evol. 31 (2014) 1077–1088, https://doi.org/10.1093/MOLBEV/MSU088.

[19] T. Seemann, Prokka: rapid prokaryotic genome annotation, Bioinformatics 30 (2014) 2068–2069, https://doi.org/10.1093/BIOINFORMATICS/BTU153.

[20] A. Gurevich, V. Saveliev, N. Vyahhi, G. Tesler, QUAST: Quality assessment tool for genome assemblies, Bioinformatics 29 (2013) 1072–1075, https://doi.org/10.1093/BIOINFORMATICS/BTT086.

[21] C.M. Camilo, I. Polikarpov, High-throughput cloning, expression and purification of glycoside hydrolases using Ligation-Independent Cloning (LIC), Protein Expr. Purif. 99 (2014) 35–42, https://doi.org/10.1016/j.pep.2014.03.008.

[22] M. Michikawa, H. Ichinose, M. Momma, P. Biely, S. Jongkees, M. Yoshida, T. Kotake, Y. Tsumuraya, S.G. Withers, Z. Fujimoto, S. Kaneko, Structural and biochemical characterization of glycoside hydrolase family 79 β-Glucuronidase from acidobacterium capsulatum, J. Biol. Chem. 287 (2012) 14069, https://doi.org/10.1074/JBC.M112.346288.

[23] S. Pengthaisong, B. Piniello, G.J. Davies, C. Rovira, J.R. Ketudat Cairns, Reaction mechanism of glycoside hydrolase family 116 utilizes perpendicular protonation, ACS Catal. 13 (2023) 5850–5863, https://doi.org/10.1021/ACSCATAL.3C00620.

[24] J. Gao, W. Wakarchuk, Characterization of Five β-glycoside hydrolases from cellulomonas fimi ATCC 484, J. Bacteriol. 196 (2014) 4103–4110, https://doi.org/10.1128/JB.02194-14.

[25] Y.L. Jiang, W.L. Yu, J.W. Zhang, C. Frolet, A.M. Di Guilmi, C.Z. Zhou, T. Vernet, Y. Chen, Structural basis for the substrate specificity of a novel β-N-Acetylhexosaminidase StrH Protein from Streptococcus pneumoniae R6, J. Biol. Chem. 286 (2011) 43004, https://doi.org/10.1074/JBC.M111.256578.

[26] M. Mirdita, K. Schütze, Y. Moriwaki, L. Heo, S. Ovchinnikov, M. Steinegger, ColabFold: making protein folding accessible to all, Nat. Methods 19 (2022) 679–682, https://doi.org/10.1038/S41592-022-01488-1;SUBJMETA=114,129,2044,2397,2411,631,794;KWRD=COMPUTATIONAL+MODELS,PROTEIN+DATABASES,PROTEIN+STRUCTURE+PREDICTIONS,SOFTWARE.

[27] N. Ramasubbu, L.M. Thomas, C. Ragunath, J.B. Kaplan, Structural Analysis of Dispersin B, a Biofilm-releasing Glycoside Hydrolase from the Periodontopathogen Actinobacillus actinomycetemcomitans, J. Mol. Biol. 349 (2005) 475–486, https://doi.org/10.1016/J.JMB.2005.03.082.

[28] S. Kumar, G. Stecher, M. Li, C. Knyaz, K. Tamura, X. MEGA, Molecular evolutionary genetics analysis across computing platforms, Mol. Biol. Evol. 35 (2018) 1547–1549, https://doi.org/10.1093/MOLBEV/MSY096.

[29] P. Gouet, X. Robert, E. Courcelle, ESPript/ENDscript: Extracting and rendering sequence and 3D information from atomic structures of proteins, Nucleic. Acids. Res. 31 (2003) 3320–3323, https://doi.org/10.1093/NAR/GKG556.

[30] P. Costa, A.T.P.C. Gomes, M. Braz, C. Pereira, A. Almeida, Application of the resazurin cell viability assay to monitor escherichia coli and salmonella typhimurium inactivation mediated by phages, Antibiot. (Basel) (2021) 10, https://doi.org/10.3390/ANTIBIOTICS10080974.

[31] L.V.B. Samaniego, S.L. Scandelau, C.R. Silva, S. Pratavieira, V. de Oliveira Arnoldi Pellegrini, A.N.G. Dabul, L.A. Esmerino, M. de Oliveira Neto, R.T. Hernandes, F. Segato, M. Pileggi, I. Polikarpov, Thermothelomyces thermophilus exo- and endo-glucanases as tools for pathogenic E. coli biofilm degradation, Sci. Rep. 14 (2024) 1–18, https://doi.org/10.1038/S41598-024-70144-9;SUBJMETA=22,326,338,45,46,603,61,631;KWRD=ANTIMICROBIALS,BIOCATALYSIS,BIOFILMS.

[32] S.M. Kwong, J.P. Ramsay, S.O. Jensen, N. Firth, Replication of staphylococcal resistance plasmids, Front. Microbiol. 8 (2017) 316207, https://doi.org/10.3389/FMICB.2017.02279/BIBTEX.

[33] A.P. Breslawec, S. Wang, C. Li, M.B. Poulin, Anionic amino acids support hydrolysis of poly-β-(1,6)-N-acetylglucosamine exopolysaccharides by the biofilm dispersing

glycosidase Dispersin B, J. Biol. Chem. 296 (2021) 100203, https://doi.org/10.1074/JBC.RA120.015524.
[34] S.G.A. Manuel, C. Ragunath, H.B.R. Sait, E.A. Izano, J.B. Kaplan, N. Ramasubbu, Role of active-site residues of dispersin B, a biofilm-releasing β-hexosaminidase from a periodontal pathogen, in substrate hydrolysis, FEBS J. 274 (2007) 5987–5999, https://doi.org/10.1111/J.1742-4658.2007.06121.X.
[35] T. Liu, Y. Duan, Q. Yang, Revisiting glycoside hydrolase family 20 β-N-acetyl-D-hexosaminidases: crystal structures, physiological substrates and specific inhibitors, Biotechnol. Adv. 36 (2018) 1127–1138, https://doi.org/10.1016/J.BIOTECHADV.2018.03.013.
[36] P. Neopane, H.P. Nepal, R. Shrestha, O. Uehara, Y. Abiko, In vitro biofilm formation by Staphylococcus aureus isolated from wounds of hospital-admitted patients and their association with antimicrobial resistance, Int. J. Gen. Med. 11 (2018) 25–32, https://doi.org/10.2147/IJGM.S153268.
[37] C.E. Fidelis, A.M. Orsi, G. Freu, J.L. Gonçalves, M.V. dos Santos, Biofilm formation and antimicrobial resistance of Staphylococcus aureus and Streptococcus uberis Isolates from bovine mastitis, Vet. Sci. 11 (2024), https://doi.org/10.3390/VETSCI11040170.
[38] B. Campos, A.C. Pickering, L.S. Rocha, A.P. Aguilar, M.H. Fabres-Klein, T.A. de Oliveira Mendes, J.R. Fitzgerald, A. de Oliveira Barros Ribon, Diversity and pathogenesis of Staphylococcus aureus from bovine mastitis: current understanding and future perspectives, BMC Vet. Res. 18 (1 18) (2022) 1–16, https://doi.org/10.1186/S12917-022-03197-5, 2022.
[39] B.A. Diep, S.R. Gill, R.F. Chang, T.H. Van Phan, J.H. Chen, M.G. Davidson, F. Lin, J. Lin, H.A. Carleton, E.F. Mongodin, G.F. Sensabaugh, F. Perdreau-Remington, Complete genome sequence of USA300, an epidemic clone of community-acquired meticillin-resistant Staphylococcus aureus, Lancet 367 (2006) 731–739, https://doi.org/10.1016/S0140-6736(06)68231-7.
[40] M.F. Augusto, D.C. da Silva Fernandes, T.L.R. de Oliveira, F.S. Cavalcante, R. C. Chamon, A.L.P. Ferreira, S.A. Nouér, A.P. Rangel, A.C. Castiñeiras, C. M. Gonçalez, J. Freire, L.F. Guimarães, R. Batista, K.R.N. dos Santos, Pandemic clone USA300 in a Brazilian hospital: detection of an emergent lineage among methicillin-resistant Staphylococcus aureus isolates from bloodstream infections, Antimicrob. Resist. Infect. Control 11 (2022) 114, https://doi.org/10.1186/S13756-022-01154-3.
[41] N.C. Silva, M.C. de Souza, M.A.L. Tonini, R.P. Schuenck, Dissemination of methicillin-resistant Staphylococcus aureus USA300 ST8/PVL- positive in breast infections in a Brazilian region, Diagn. Microbiol. Infect. Dis. 106 (2023) 115919, https://doi.org/10.1016/J.DIAGMICROBIO.2023.115919.
[42] C. de O. Whitaker, R.C. Chamon, T.L.R. de Oliveira, S.A. Nouér, K.R.N. dos Santos, Systemic infection caused by the methicillin-resistant Staphylococcus aureus USA300-LV lineage in a Brazilian child previously colonized, Braz. J. Infect. Dis. 27 (2023) 102737, https://doi.org/10.1016/J.BJID.2022.102737.
[43] Z. Zhu, Z. Hu, S. Li, R. Fang, H.K. Ono, D.L. Hu, Molecular Characteristics and Pathogenicity of Staphylococcus aureus Exotoxins, Int. J. Mol. Sci. 25 (2024) 395, https://doi.org/10.3390/IJMS25010395. Page25 (2023) 395.
[44] B.D. Gimza, M.I. Larias, B.G. Budny, L.N. Shaw, Mapping the global network of extracellular protease regulation in Staphylococcus aureus, MSphere 4 (2019) e00676, https://doi.org/10.1128/MSPHERE.00676-19. -19.
[45] B.D. Gimza, J.K. Jackson, A.M. Frey, B.G. Budny, D. Chaput, D.N. Rizzo, L.N. Shaw, Unraveling the impact of secreted proteases on hypervirulence in Staphylococcus aureus, mBio 12 (2021) 1–15, https://doi.org/10.1128/MBIO.03288-20.
[46] A.M.S. Figueiredo, F.A. Ferreira, C.O. Beltrame, M.F. Côrtes, The role of biofilms in persistent infections and factors involved in ica-independent biofilm development and gene regulation in Staphylococcus aureus, Crit. Rev. Microbiol. 43 (2017) 602–620, https://doi.org/10.1080/1040841X.2017.1282941.
[47] A. Toledo-Arana, N. Merino, M. Vergara-Irigaray, M. Débarbouillé, J.R. Penadés, I. Lasa, Staphylococcus aureus develops an alternative, ica-independent biofilm in the absence of the arlRS two-component system, J. Bacteriol. 187 (2005) 5318, https://doi.org/10.1128/JB.187.15.5318-5329.2005.
[48] Q. Peng, X. Tang, W. Dong, N. Sun, W. Yuan, A Review of biofilm formation of Staphylococcus aureus and its regulation mechanism, Antibiotics 12 (2022) 12, https://doi.org/10.3390/ANTIBIOTICS12010012.
[49] B. Schwartbeck, C.H. Rumpf, R.J. Hait, T. Janssen, S. Deiwick, V. Schwierzeck, A. Mellmann, B.C. Kahl, Various mutations in icaR, the repressor of the icaADBC locus, occur in mucoid Staphylococcus aureus isolates recovered from the airways of people with cystic fibrosis, Microbes. Infect. 26 (2024) 105306, https://doi.org/10.1016/J.MICINF.2024.105306.
[50] B. Pluvinage, M.A. Higgins, D.W. Abbott, C. Robb, A.B. Dalia, L. Deng, J.N. Weiser, T.B. Parsons, A.J. Fairbanks, D.J. Vocadlo, A.B. Boraston, Inhibition of the pneumococcal virulence factor StrH and molecular insights into N-glycan recognition and hydrolysis, Structure 19 (2011) 1603–1614, https://doi.org/10.1016/J.STR.2011.08.011.
[51] B.L. Mark, D.J. Vocadlo, D. Zhao, S. Knapp, S.G. Withers, M.N.G. James, Biochemical and structural assessment of the 1-N-Azasugar GalNAc-isofagomine as a potent family 20 β-N-acetylhexosaminidase inhibitor, J. Biol. Chem. 276 (2001) 42131–42137, https://doi.org/10.1074/jbc.m107154200.
[52] J.B. Kaplan, C. Cywes-Bentley, G.B. Pier, N. Yakandawala, M. Sailer, M.S. Edwards, K. Kridin, Poly-β-(1→6)-N-acetyl-D-glucosamine mediates surface attachment, biofilm formation, and biocide resistance in Cutibacterium acnes, Front. Microbiol. 15 (2024) 1386017, https://doi.org/10.3389/FMICB.2024.1386017/BIBTEX.
[53] H. Poilvache, A. Ruiz-Sorribas, O. Cornu, F. van Bambeke, In vitro study of the synergistic effect of an enzyme cocktail and antibiotics against biofilms in a prosthetic joint infection model, Antimicrob. Agents Chemother 65 (2021), https://doi.org/10.1128/AAC.01699-20/SUPPL_FILE/AAC.01699-20-S0001.PDF.
[54] E. Kamali, A. Jamali, A. Izanloo, A. Ardebili, In vitro activities of cellulase and ceftazidime, alone and in combination against Pseudomonas aeruginosa biofilms, BMC. Microbiol. 21 (2021) 1–10, https://doi.org/10.1186/S12866-021-02411-Y/TABLES/3.
[55] M. Anderson, D. Panteli, R. van Kessel, G. Ljungqvist, F. Colombo, E. Mossialos, Challenges and opportunities for incentivising antibiotic research and development in Europe, Lancet Reg. Health - Eur. 33 (2023) 100705, https://doi.org/10.1016/J.LANEPE.2023.100705.
[56] H. Brüssow, The antibiotic resistance crisis and the development of new antibiotics, Microb. Biotechnol. 17 (2024), https://doi.org/10.1111/1751-7915.14510.